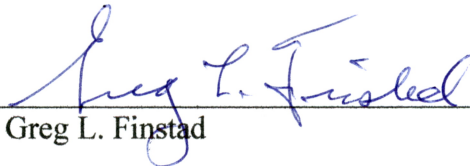


CHARACTERIZATION AND DELINEATION OF CARIBOU HABITAT ON UNIMAK
ISLAND USING REMOTE SENSING TECHNIQUES


By

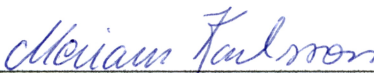
Brian M. Atkinson

RECOMMENDED:

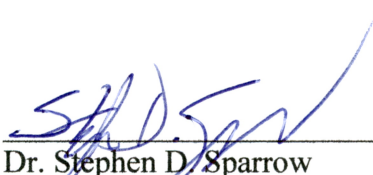

Dr. Greg L. Finstad

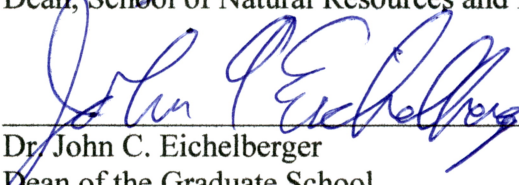

Dr. David L. Verbyla

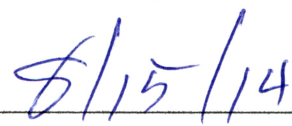

Dr. Norman R. Harris
Advisory Committee Chair


Dr. Meriam G. Karlsson
Chair, High Latitude Agriculture

APPROVED:


Dr. Stephen D. Sparrow
Dean, School of Natural Resources and Extension


Dr. John C. Eichelberger
Dean of the Graduate School


Date

CHARACTERIZATION AND DELINEATION OF CARIBOU HABITAT ON UNIMAK
ISLAND USING REMOTE SENSING TECHNIQUES

A
THESIS

Presented to the Faculty
of the University of Alaska Fairbanks

in Partial Fulfillment of the Requirements
for the Degree of
MASTER OF SCIENCE

By

Brian M. Atkinson, B.S.

Fairbanks, Alaska

August 2014

ABSTRACT

The assessment of herbivore habitat quality is traditionally based on quantifying the forages available to the animal across their home range through ground-based techniques. While these methods are highly accurate, they can be time-consuming and highly expensive, especially for herbivores that occupy vast spatial landscapes. The Unimak Island caribou herd has been decreasing in the last decade at rates that have prompted discussion of management intervention. Frequent inclement weather in this region of Alaska has provided for little opportunity to study the caribou forage habitat on Unimak Island. The overall objectives of this study were two-fold 1) to assess the feasibility of using high-resolution color and near-infrared aerial imagery to map the forage distribution of caribou habitat on Unimak Island and 2) to assess the use of a new high-resolution multispectral satellite imagery platform, RapidEye, and use of the “red-edge” spectral band on vegetation classification accuracy. Maximum likelihood classification algorithms were used to create land cover maps in aerial and satellite imagery. Accuracy assessments and transformed divergence values were produced to assess vegetative spectral information and classification accuracy. By using RapidEye and aerial digital imagery in a hierarchical supervised classification technique, we were able to produce a high resolution land cover map of Unimak Island. We obtained overall accuracy rates of 71.4 percent which are comparable to other land cover maps using RapidEye imagery. The “red-edge” spectral band included in the RapidEye imagery provides additional spectral information that allows for a more accurate overall classification, raising overall accuracy 5.2 percent.

TABLE OF CONTENTS

	Page
Signature Page	i
Title Page	iii
Abstract	v
Table of Contents	vii
List of Figures	xi
List of Tables	xiii
Acknowledgements	xv
General Introduction	1
CHAPTER 1: High Resolution Multispectral Aerial Photography to Delineate and Assess Temporal Phenology of Caribou Habitat on Unimak Island	3
Abstract	3
Introduction	5
Decline of Caribou	5
Land Cover Determination	6
Methods	8
Study Site Description	8
Aerial Digital Imagery	12
Ground-Truthing	14
Image Processing	15
Image Classification	17

	Page
Accuracy Assessment	18
Results	19
Vegetation Community Composition	19
Accuracy Assessment	20
Discussion	25
Future Research Areas	26
Literature Cited	28
CHAPTER 2: High Resolution Satellite Imagery to Quantify and Delineate Caribou Habitat on Unimak Island	31
Abstract	31
Introduction	33
Decline of Caribou	33
Land Cover Determination	34
Methods	36
Study Site Description	36
Satellite Imagery	40
Training Sites/Ground Truthing	41
Ground-Truthing	42
Unsupervised and Supervised Classification Methods	43
Accuracy Assessment	44
Red-edge Spectral Band Assessment	44
Comparison to NLCD	46

	Page
Results.....	47
Accuracy Assessment	50
Red-edge Spectral Band Assessment.....	53
Comparison to NLCD	56
Discussion	60
Red-edge Spectral Band Assessment.....	61
Comparison to NLCD	62
Implications.....	63
Improvements and Future Research Areas	63
Literature Cited	65
General Conclusions	69
Literature Cited	72
Appendix.....	75

LIST OF FIGURES

	Page
Figure 1.1 Examples of color, near-infrared and near-infrared “hot-spot” of aerial imagery	16
Figure 1.2 USGS Digital raster graphic of study site, Unimak Island, Alaska.....	8
Figure 1.3 Canopy cover percentage by vegetative community type	20
Figure 1.4 Spring, summer and fall comparisons of mean digital reflectance value by spectral band for select vegetation classes.	22
Figure 1.5 Maximum likelihood supervised classification from a single area from three dates of aerial imagery; spring, summer and fall	25
Figure 2.1 RapidEye color image of a subset of Unimak Island	38
Figure 2.3 RapidEye maximum likelihood classification image of Unimak Island	49
Figure 2.3 Spectral response patterns for 4 vegetative classes in the RapidEye maximum likelihood classification	53
Figure 2.4 Producer's accuracy rate (%) for 7 vegetation classes between 4 RapidEye composite classifications.....	54
Figure 2.5 Overview of the NLCD and RapidEye land cover maps	57
Figure 2.6 Comparison of RapidEye and Landsat NLCD land cover maps	58
Figure 2.7 Image difference between Rapideye and NLCD land cover maps.....	60

LIST OF TABLES

	Page
Table 1.1 Phenological plant stage and corresponding dates of aerial photography	13
Table 1.2 Average, minimum and select pairwise transformed divergence values for vegetation classes.	21
Table 1.3 Average transformed divergence values by imagery acquisition date for vegetation classes	23
Table 1.4 Overall and vegetation classification accuracies and Kappa statistic for 3 dates of aerial imagery acquisition	23
Table 1.5 Producer's and user's accuracy for sedge, willow, alder and mixed forb communities.	24
Table 2.1 List of RapidEye composite images used to assess the red-edge band	46
Table 2.2 Areal coverage of land cover classes in hectares from the RapidEye maximum likelihood classification	48
Table 2.3 Overall accuracy and kappa statistic for the RapidEye maximum likelihood classification	50
Table 2.4 Producer's accuracy, user's accuracy, and kappa statistic for vegetative community types	50
Table 2.5 Transformed divergence value matrix for vegetative land cover classes	52
Table 2.6 Error matrix showing classification accuracy and misclassification rate by class	52
Table 2.7 Comparison of overall classification accuracy and Kappa statistic for 4 RapidEye composite classifications	53
Table 2.8 User's and producer's accuracy rate comparison between RapidEye and RapidEye – RE composite image	55
Table 2.9 Transformed divergence spectral separability values for 4 RapidEye composite classificaions	55
Table 2.10 Transformed divergence values by band for select vegetative class comparisons in the original RapidEye classification	56
Table 2.11 Overall classification accuracy and kappa statistics for the RapidEye and NLCD land cover maps	56

	Page
Table 2.12 Areal coverage of shared land cover classes in RapidEye and NLCD land cover maps	59
Table A-1 Vegetative pairwise comparison of transformed divergence values by spectral band for Rapideye classification map.....	75
Table A-2 Classification matrix (%) of NLCD class areas in common with RapidEye land cover map.....	75
Table A-3 Classification matrix (hectares) of NLCD class areas in common with RapidEye land cover map.....	76

ACKNOWLEDGEMENTS

First and foremost I would like to thank my major advisor, Dr. Norman Harris, for all of the guidance, suggestions and support in this project. It would not have been possible without his knowledge and assistance with everything from field logistics to the editing of my thesis. I would also like to thank him for allowing me to take on this project, as I had little to no experience with remote sensing or GIS when first signing on to the project. I also thank my committee members Dr. Greg Finstad and Dr. David Verbyla for their help with thesis edits and helpful suggestions throughout the project.

I would also like to thank Dr. Don Spalinger, Dr. William Collins, and Dr. Christine Peterson for all of their help with the initial field set-up, logistics, thesis edits, brain-storming sessions and everything in between. I thank our field pilots, Kevin Fox, Chuck Moore, William Lawrence, Troy Cambier, and Mark Packala for their expert flying skills in transporting supplies and field crew, obtaining aerial photography, and even going outside of their job description to help with plant sampling and field-camp set-up. Thank you to the Izembek National Wildlife Refuge, all of its employees, including Nancy Hoffman, Leticia Melendez, Stacey Lowe, Franz Muller, and Catherine Bland for assisting with housing and always being available for all of our project needs.

I would also like to thank the U.S. Fish and Wildlife Service, the Alaska Department of Fish and Game, UAF, UAA, and the Center for Global Change at UAF for funding this project. I would like to thank my partner on the project, Kate Legner for the support and guidance she has provided through every aspect of this study. Finally, I would like to thank all of my family and friends that have supported me throughout the entirety of this project.

GENERAL INTRODUCTION

The population dynamics of caribou are regulated by many environmental factors. These include bottom-up constraints, such as forage nutritional quality and quantity limitations as influenced by general weather patterns and soil conditions, and top-down constraints, such as predation, insects/parasites, disease and extreme weather events (Klein, 1991; McArt et al., 2009; Sæther, 1997). All of these factors can influence population dynamics both indirectly or directly through reduced body condition and reproductive success, calf recruitment and survival, overwinter survival rate, and many other factors.

Caribou (*Rangifer tarandus*) populations have been declining throughout the world (Vors & Boyce, 2009) at a rate that has prompted concerns about population longevity. Large ungulate populations are known to fluctuate through time (Klein, 1991; Valkenburg et al., 2003), but the concurrent decline of caribou herds around the world has caused many to suspect climate change as a regulating factor in these herds (Heggberget et al., 2010; Tyler, 2010; Vors & Boyce, 2009). Theories about climate warming effects proposed to date include the increased occurrence of freeze-thaw cycles that lock vital winter forage under layers of ice (Heggberget et al., 2010; Stien et al., 2010; Tyler, 2010), and also a process termed trophic mismatch (Post & Forchhammer, 2008; Post et al., 2008); the increased variability in spatiotemporal availability of nutritious plants following spring green-up.

These trends of concurrent population decline have also been observed for many caribou herds throughout Alaska (Vors & Boyce, 2009). The Unimak Island caribou herd in southwestern Alaska is one such herd and it has experienced a population decline of two-thirds between the years of 2002-2009 (U.S. Fish and Wildlife Service, 2010). The population has dropped from a high of 1,261 animals to the present estimated low of 200 (Dale et al., 2013).

This decline has been coupled with decreases in the natality rate (85%, 2008/09, to 70 % , 2012/13), calf to cow ratio (21:100, 2000/01, to 3:100, 2012/2013), and bull to cow ratio (a high of 54:100 in 2002 to a present low of 6:100 in 2011) (Dale et al., 2013). While the Unimak Island caribou herd population may fluctuate on a 40-50 year cycle (Valkenburg et al., 2003), concern over its continued sharp decline has led to discussion of management intervention, in the form of predator control, in an attempt to prevent the extinction of this distinct population (U.S. Fish and Wildlife Service, 2010). Proposed control measures have been controversial since little is known about Unimak Island in the regards to caribou forage, composition and suitability, and habitat, principally because of the isolation, remoteness and extreme weather of this region (Valkenburg et al., 2003).

While wolf and brown bear predation have been shown to be a major factor in reducing populations of other southwestern caribou herds (Dale et al., 2013; U.S. Fish and Wildlife Service, 2010), little is known about forage quality, quantity and nutritional suitability for this herd. In order to evaluate habitat quality and to quantify forage availability to the Unimak Island caribou herd, a remote sensing study was undertaken to map vegetative communities for the entirety of Unimak Island. The key objectives of this study were 1) to perform and evaluate low-level high-resolution aerial photography for detailed mapping of caribou forage, and 2) to evaluate a relatively new high-resolution satellite platform, RapidEye, for the delineation of caribou forage in southwestern Alaska.

CHAPTER 1: HIGH RESOLUTION MULTISPECTRAL AERIAL PHOTOGRAPHY TO DELINEATE AND ASSESS TEMPORAL PHENOLOGY OF CARIBOU HABITAT ON UNIMAK ISLAND¹

ABSTRACT

The assessment of herbivore habitat is traditionally based on quantifying the forages available to the animal across their home range and the nutritional quality of those forages through ground-based methods. While these methods are highly accurate and useful, they can be time-consuming and expensive. Because of the difficulty in evaluating habitat across large spatial scales, remote sensing is often employed as a tool to map forage. The goal of this study was to assess the feasibility of using high-resolution color and near-infrared aerial photography to map the distribution of summer forage for caribou on Unimak Island in southwestern Alaska. Aerial photos were taken on June 11 and 13, 2011, July 3 and 7, 2011, and September 17, 2011, corresponding to early spring, summer, and fall during the growing season. These images were classified using a maximum likelihood classification in ERDAS Imagine[®]. Accuracy assessments of the classified images were conducted to determine the best timing for this aerial photography-based classification technique. Transformed divergence values were calculated to assess the effect of plant phenology on the spectral response pattern and to determine the separability of key plant communities during the three sampling periods. It was also used to assess the separability of individual spectral bands. Summer dates of aerial photography had the highest accuracy rate (84%), followed by fall (78%) and spring (78%). Overall transformed

divergence values were the highest for summer, followed by fall and spring, indicating that summer provided the best time period for spectral separability and vegetation classification.

INTRODUCTION

Decline of Caribou

Caribou (*Rangifer tarandus*) populations have been declining throughout the world (Vors & Boyce, 2009) at a rate that has prompted concerns about population longevity. These trends of population decline have also been observed for many caribou herds throughout Alaska (Valkenburg et al., 2003, U.S. Fish and Wildlife Service 2010). The Unimak Island caribou herd in southwest Alaska is one such herd, and its continued sharp decline over the past decade has prompted discussion of drastic intervention in an attempt to prevent the extinction of this population (U.S. Fish and Wildlife Service 2010).

While wolves and brown bears are known to predate on calves on Unimak Island, and have limited calf recruitment in other nearby herds on the Southern Alaska Peninsula (Dale et al., 2013; U.S. Fish and Wildlife Service, 2010), the role of forage quality and quantity on the Unimak Island caribou herd is not understood. Forage quality is related to the multiple factors, but for large herbivores generally includes whether the forage protein content and the digestibility of the forage are adequate to sustain population growth or individual physiologic processes. Many environmental factors, particularly weather and climate related, greatly influence the growth of forage plants and their subsequent quality, through direct and indirect effects. Due to the trends of circumpolar decline of caribou herds, several global climate change/forage quality relationships have been proposed that may influence caribou population dynamics. These include the increased occurrence of freeze-thaw cycles that lock vital winter forage under layers of ice (Heggberget et al., 2010; Stien et al., 2010; Tyler, 2010), and also a process termed trophic mismatch (Post & Forchhammer, 2008; Post et al., 2008). In order to

evaluate the quality of caribou habitat and potential climate change effects on caribou habitat, an assessment of the spatial distribution of forage species is required.

Land Cover Determination

The management of large herbivores generally requires an accurate assessment of the forages that are available to that herbivore, both spatially and temporally (Mårell & Edenius, 2006). In order to assess habitat quality, an estimate of available forage and quality is needed (Trudell & White, 1981). Traditionally, this was accomplished through the use of hand clip plots to estimate forage biomass and nutritional quality. Estimating the available forage can be difficult because of the large area that an animal can occupy as its habitat. This is especially true for migratory animals such as caribou (*Rangifer tarandus*) that can migrate thousands of kilometers annually and have a home range of thousands of square kilometers (Fancy et al., 1989). Remote sensing and the use of land cover maps have become an important tool for land managers wishing to determine the distribution of forage plants for large herbivores. A land cover map can provide the basic spatial coverage and distribution of vegetative communities over a very large area. This map can be coupled with biomass estimates to give an approximate idea of forage production, and with nutritional information to provide a habitat quality assessment.

Remote sensing through the use of various detectors of electromagnetic energy has proven to be an efficient and effective means of quantifying vegetative traits across vast landscapes. The advancement of remote sensing techniques over the last two decades has allowed for the detection of a variety of canopy biochemistry characteristics (Kokaly et al., 2009; Ustin et al., 2009), and increased accuracy of classification of vegetation communities (Xie et al.,

2008). Remote sensing has been widely adapted for use in ecology and has proven to be very useful in large-area mapping and assessment of habitat (Cohen & Goward, 2004).

The spatial distribution of forage is an important aspect for habitat assessment and management of large herbivores (Gordon et al., 2004). Unfortunately, this can prove difficult to evaluate because of the hierarchal scale of foraging; areas that herbivores utilize can range from small foraging sites of a single forage species, up to large heterogeneous plant community landscapes composed of many individual vegetative communities (Johnson et al., 2002; Johnson et al., 2001; Shipley & Spalinger, 1992) The use of remote sensing techniques addresses this issue by allowing for a plant community resolution with landscape scale coverage. There are many examples of the use of remote sensing for evaluating caribou habitat. Johnson (2003) successfully mapped 27 vegetation types across boreal and sub-boreal caribou habitat in northcentral British Columbia, Canada using Landsat TM imagery and ancillary GIS data. Théau et al. (2005) also used Landsat TM imagery and two classification methods to map lichen abundance, an important winter forage of caribou, in northern Quebec, Canada. Hansen et al. (2001) utilized both Landsat MSS and Landsat TM imagery to evaluate land cover change and habitat fragmentation for mountain caribou habitat range in British Columbia, Canada. Finally, Bartsch et al. (2010) was able to correlate observed rain-on-snow events and the subsequent formation of ice layers on caribou winter range using backscatter data from the QuikSCAT scatterometer. Clearly, remote sensing has many uses in caribou habitat assessment, largely due to the fact that migrating herds occupy vast landscapes and remote sensing allows for effective evaluation and monitoring of the habitat. Unfortunately, remote sensing data usually are not detailed enough at the ground level to distinguish fine differences in habitat types, due to the low spatial resolution of the imagery. Current widespread imagery typically used for land cover maps

is from the Landsat program. This spectral data has a spatial resolution of 30 meters on a side. While this can allow for broad community type classifications, it often fails to detect vegetation communities of a smaller size that are often of high nutritional importance.

While Landsat imagery is available for Unimak Island, it is limited seasonally by the high cloud cover over the Aleutian Islands and the Southern Alaska Peninsula. Due to this and the extreme weather and remoteness of the area, little is known about this herd or its habitat (Valkenburg et al., 2003). In order to address the lack of knowledge about caribou forage distribution on Unimak Island, we proposed to develop and assess remote sensing techniques to produce land cover maps using low-level high-resolution aerial photography. Our goals for this study were two-part, 1) to assess the application and accuracy of low-level high-resolution aerial imagery for a detailed approach to caribou forage distribution mapping on Unimak Island and 2) to determine the best seasonal period to obtain imagery for use with remote sensing on Unimak Island.

METHODS

Study Site Description

Unimak Island (Figure 1.1) (54.7683° N, -164.1867° W) is a volcanic island that lies at the easternmost end of the Aleutian Island Archipelago in southwestern Alaska. Its land area is approximately 4,070 km² and it is the largest of the 69 Aleutian Islands. Located in the center of Unimak Island is Mount Shishaldin, one of the most active volcanoes in the world. Weather on Unimak Island is characterized by moderate temperatures both in summer and winter due to the moderation caused by the coastal current and air patterns. The Aleutian area is often referred to as the “Cradle of the Storms”, a colloquial term that refers to the a low pressure system that is

centered near Unimak Island and the Southern Alaska Peninsula, and is generally thought of as the stormiest area in the North Pacific. Cold water and air from the north, originating in the Bering Sea, meets the warmer water and air from the south in the Gulf of Alaska to create the frequent extreme weather of the Alaska Peninsula. The most reliable source of weather data is from the city of Cold Bay, Alaska, approximately 70 kilometers from Unimak Island. Average monthly air temperature varies only approximately 13°C between summer and winter months, ranging from -2°C in January to 11°C in August. Average daily wind speeds are the highest for any area in the United States, at 13.5 knots. Annual precipitation is approximately 97 centimeters, with the most precipitation coming in the winter months. Snowfall averages 155 centimeters per year, with snow depth averaging 5 to 10 centimeters for the months of December through April. Rain-on-snow and thaw-refreeze events are the most prevalent here in the state of Alaska, and average greater than 7 events per year (Wilson et al., 2013).



Figure 1.1 USGS Digital raster graphic of study site, Unimak Island, Alaska. The upper-left subset graphic is a reference image of Alaska, and indicates the geographic location of Unimak Island with respect to Alaska.

Unimak Island is separated from the southern tip of the Alaska Peninsula by the narrow Isanotski Strait, which is approximately 700 meters wide. This narrow strait has allowed for populations of caribou (*Rangifer tarandus*), brown bear (*Ursus arctos*), wolf (*Canis lupis*), and red fox (*Vulpes vulpes*) to occasionally cross to the island. Hence, it is the only Aleutian Island with naturally occurring populations of these fauna (U.S. Fish and Wildlife Service, 2010).

Unimak Island is classified as a marine tundra environment and is characterized by the absence of trees, large areas of barren ground from geologically-recent volcanic activity and high winds, and a sharp increase in elevation, from sea level to 2,857 meters (Mount Shishaldin), in just over 14 kilometers. Other volcanoes include Pogromni, Isanotski, and Roundtop. Geologic deposits consist of glacial till and outwash from the late Wisconsin glacial period, and frequent ash and lava deposits. Beach sediment deposits and dune formation are also common on the north side of Unimak Island along the coast. Soils on Unimak Island are relatively young and are, most likely, volcanic ash dominated Andisols, poorly developed Entisols and Inceptisols, and poorly drained Histosols (Wilson, Miller, and Detterman, 1992).

Dominant vegetation community types across the island include dwarf-shrub crowberry tundra heath (*Empetrum nigrum*), sedge meadows (*Carex spp.*), tall-shrub alder (*Alnus crispa*), low-shrub willow (*Salix spp.*), herbaceous species (Talbot et al., 2006). The sharp elevation gradient on Unimak Island also provides for two distinct tundra types, here defined as lowland and upland tundra. Upland tundra sites tend to be composed of the same species, but green-up in the spring is delayed to differences in temperature due to the elevation gradient. Upland tundra sites also appear to have healthier *Empetrum nigrum* stands; lowland tundra sites had a widespread characteristic of dead or non-photosynthetically active plants. Definitions of

vegetative community cover types followed a modified Viereck Alaska Vegetation Classification system (Viereck et al., 1992). Each major vegetative community type was assigned to a level IV classification. Classes following this system included low-scrub willow, tall shrub alder, herbaceous graminoid – wet (emergent wetlands), mixed herbaceous communities, and dwarf scrub empetrum tundra. For our purposes, a dominant vegetation type is defined as a plant community where the clear majority of species present on an area basis are of one plant species. This distinction allows for broader classification of vegetation species into groups. While we evaluated the entire island and all of its vegetative community types, caribou are known to only forage on a few species found on Unimak Island. These forage types generally consist of forbs, grasses and sedges, and shrubs within the genus *Salix* (White, 1983; White and Trudell, 1980). Caribou are not known to forage on other shrub species that occur on Unimak Island, such as *Alnus viridis*, *Arctostaphylos uva-ursi*, *Empetrum nigrum*, *Vaccinium uliginosum*, and *V. vitis-idaea*. Lichen species are a major component of caribou winter diet, mainly consisting of lichens in the *Cladonia* genus. Lichen species that were found were mainly in the *Peltigera* genus, a non-forage species of caribou. No lichen communities were established for this study on Unimak Island.

Aerial Digital Imagery

Methods for obtaining and classifying aerial imagery followed that of Walton et al. (2011, 2013). High resolution digital images were taken along 55 single-line transects in areas with anecdotal evidence of high densities of caribou. These areas were mainly along the north-eastern side of the island as this was where caribou were often spotted on previous aerial surveys of the herd (William Collins, personal communication). Transects were also taken along the

western and southern side of the island but the majority of ground-truthing of aerial imagery occurred in the north-eastern area of the island because of logistical constraints. Aerial images were taken during three phenologically distinct periods of plant growth. These periods included green-up in early spring, peak-growth in mid-summer and during senescence in the fall. Imagery was taken over the summer of 2011 with supplemental imagery being taken in summer 2012. For our analysis and comparison of phenological time periods, spectral information was only extracted and used from within the 2011 growing season (Table 1.1).

Table 1.1 Phenological plant stage and corresponding dates of aerial photography.

Phenological Plant Stage	Year	Dates
Spring green-up	2011	June 11, 13
Summer/peak photosynthetic activity	2011	July 3, 7, 22
Fall Senescence	2011	Sept. 17
Spring green-up	2012	-
Summer/peak photosynthetic activity	2012	July 18, 20
Fall Senescence	2012	-

Imagery from 2012 growing season served as an additional set of ground-truthed imagery for use in accuracy assessments of the satellite imagery. Each transect consisted of 20-25 photographs covering a distance of approximately 3 km. Color images were taken with a Canon EOS Rebel T2i 18.0 Megapixel camera with an EF-S 18mm lens with a UV filter. Near-infrared images were taken with the same model camera modified for capturing infrared (LDP LLC, 2014) outfitted with the same lens and a Tiffen[®] 85C infrared filter. Infrared and color images were taken at an altitude of approximately 150 meters through the belly port of a Found[®] Bush Hawk XP fixed-wing plane in 2011 and from the strut of a R44 helicopter in 2012. Images taken at this altitude cover an area approximately 185 by 125 meters with a resolution of 3.5 cm on a side.

Ground-Truthing

Selected aerial photographs from the beginning, middle, and end point of each transect were ground-truthed using a Trimble® Pathfinder Pro XR™ backpack GPS unit or a Trimble® Geo XT™ handheld GPS unit. The selection of images that were ground-truthed was based on feasibility of getting to photographed locations, and to maximize and capture variability of vegetative cover types across the island. Ground control points (GCPs) were selected based on features across the photos that were recognizable on the ground. 15 - 30 GCPs were selected per image for the initial orthorectification. GCPs were real-time corrected to the nearest base station and the majority of points had sub-meter accuracy. Points collected with the Pathfinder Pro XR GPS unit had an average horizontal accuracy of 0.4 meters and points collected with the Geo XT GPS unit had an average horizontal accuracy of 0.8 meters. Images were orthorectified in the ERDAS Imagine® LPS Project Manager using the collected GCPs, an ASTER digital elevation model (24 meter spatial resolution) of Unimak Island, and a camera model developed for our Canon T2i camera using the Photomodeler® calibration software. All images were resampled using a nearest neighborhood resampling method resulting in spatial accuracies of less than 2 meters. Images were then mosaicked using the MosaicPro tool in ERDAS Imagine® if overlapping orthorectified images were available.

Vegetation community composition was estimated for at least one vegetative community type in each ground-truthed photo to provide an estimate of vegetative ground cover across sampling locations. Vegetation canopy cover was estimated visually by use of the Daubenmire square method (Daubenmire, 1959). A 50 cm by 20 cm frame was placed at canopy level of the vegetation and each plant was identified to the species level and assigned a cover class as a percentage. A 50 meter transect was laid across a vegetation community type, and ten

Daubenmire frames were laid at five random locations along the transect resulting in 50 sampling frames per transect. Each set of ten Daubenmire frames were laid perpendicular to the transect tape, so that each set was within 2 meters of the tape. Six cover classes were used in the Daubenmire quadrant method. Canopy cover percentages for the 6 cover classes were as follows; 0-5 %, 5-25%, 25-50%, 50-75%, 75-95% and 95-100%. Canopy cover was then estimated by combining plant species into similar physiognomic plant groups and averaging and rescaling canopy cover to 100%. Vegetative canopy cover by the Daubenmire method was estimated by grouping vegetation classes into five major groups; alder-forb shrub, *empetrum nigrum* heath, mixed herbaceous, salix-forb, and sedge communities. This was done in order to create a generalized view of vegetative community composition on Unimak Island.

Image Processing

Adobe® Photoshop® CS5.1 was used to reduce image noise and coregister images. Image noise was reduced using the Reduce Noise function. A camera hotspot was evident in near-infrared images throughout all dates of photography taken. A hotspot, is the uneven illumination of an image and can be caused by many factors. Some of these factors include the uneven anomalies of lens characteristics and the attenuation of light through the lens. First the near-infrared 3-band image was converted to a Lab (Photoshop) color space. All color information was discarded by deleting the a and b color channels leaving only lightness (contrast) data. This was saved as a grayscale image. This same process was applied to an image that was taken with an ExpoDisc white balance filter, except that the spectral image information was inverted to create a “cool-spot” in the center of the image. Each near-infrared image was then masked by this “cool-spot” image whose transparency was adjusted to minimize the effects of the hot-spot.

An example of an infrared image before and after correction for the “hot-spot” is shown in Figure 1.2.

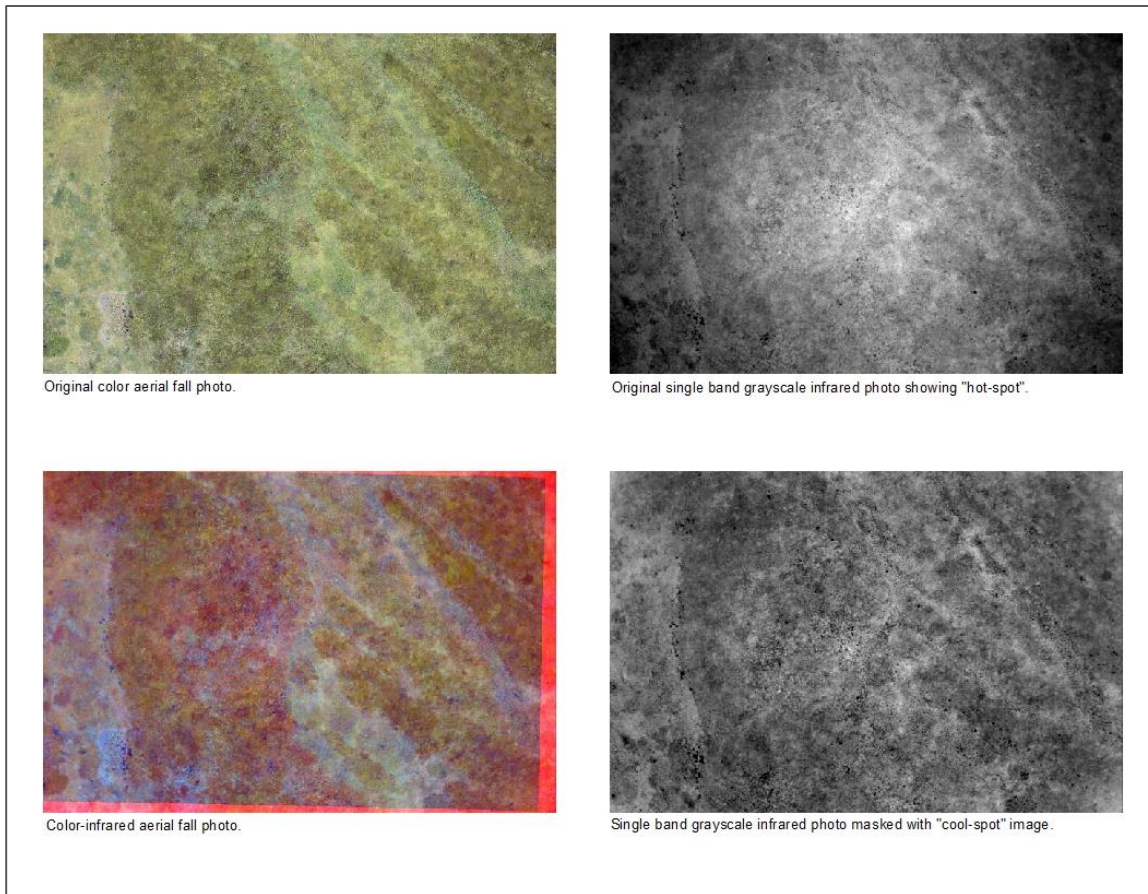


Figure 1.2 Examples of color, near-infrared and near-infrared “hot-spot” of aerial imagery. Original color photo (upper left), color-infrared photo (lower left), original infrared photo showing "hot-spot" (upper right), and masked infrared photo (lower right).

Near-infrared and color images were then manually coregistered in Photoshop[®] CS5.1 using the image transform warp and puppet warp transformation functions to create a single 4 spectral band image. Coregistration error between the color and infrared images were judged to be less than one pixel based on a pixel-level examination.

Image Classification

Supervised and unsupervised image classification methods in ERDAS Imagine[®] software were used to separate spectrally different pixels in these photos. Preliminary image classification was done with an ISODATA (iterative self-organizing data analysis technique) algorithm, the unsupervised classification routine used in Erdas. This image was used for exploratory analysis of pixel groupings. A maximum likelihood supervised classification algorithm in ERDAS Imagine[®] was used to create the final. Classes for supervised classification included open water, riverbar, rock, exposed soil, shadow, willow spp., alder, empetrum, non-photosynthetic empetrum, sedge, mixed herbaceous forb and moss spp. Training sites were established for each vegetation class in every 4-band image. A minimum of 15 training sites per vegetation class were established for each image and spectral information was extracted using those training sites. Extracted spectral information was then used as for class parameters in the maximum likelihood classification. Visual inspection of each classified image was used to assess the initial accuracy of selection of training sites.

Transformed divergence values were also calculated to give an estimate of the separability of the different vegetative communities training sites from each other. Values of 1900 and above indicate good separation between trainings groups. Values between 1700 and 1900 indicate moderately well separated values, and values below 1700 indicate poor separation. Multiple iterations and selections of training sites usually had to be performed to achieve a satisfactory classification. Once a satisfactory classification was achieved, pixels of the same thematic group were clumped using the clump function in ERDAS Imagine[®]. Pixel clumps of fewer than five pixels were then eliminated and replaced with the surrounding thematic group pixel type. This was done because specific classes within the classifications appeared to have a

“salt and pepper” appearance due to spectral variability of several vegetation classes, which introduced confusion into the final classified image.

Accuracy Assessment

Classified images from each date were combined into a single image with Adobe® Photoshop® CS5.1 creating a photo mosaic. The accuracy of the classifications was then determined by placing 250 random points across the classified photo using a stratified random sampling process with a minimum of 20 points per class. Accuracy assessments were then performed by classifying each point based on ground-truthed data and visual inspection of the original color aerial photo. A contingency table method was used to give an error matrix for the classification. Along with an estimate of overall accuracy, Producer’s and User’s accuracy were calculated. User’s accuracy reports the probability of a pixel produced in the classified map actually being located on the ground. Producer’s accuracy, reports the probability of a referenced pixel to be correctly mapped (Story and Congalton, 1986). Kappa statistics were also produced, which is an assessment of accuracy that takes into account the agreement of classification due to chance (Congalton, 1991).

RESULTS

Vegetation Community Composition

Results of the Daubenmire vegetative canopy cover estimation can be seen in Figure 1.3. One key trend to note is the common occurrence of the forb plant group across all vegetative community types located in aerial transects. Averaged across all vegetative community types, the forb class comprised 32% of all canopy cover. The canopy cover of several vegetative community types are dominated by a very few plants when plant species are grouped into similar physiognomic groups. The *Alnus viridus*/forb group was comprised of 43% alder cover and 33% forb cover. The *Empetrum nigrum* community type was dominated by *Empetrum nigrum* with over 52% of canopy cover coming from this plant species. The mixed herbaceous forb community type was dominated by the forb class, with 56% canopy cover coming from forb species. Similarly the *Carex spp.* dominated the sedge community type with over 45% of canopy cover coming from this plant group. The exception to this trend was the *Salix spp.*/forb community type, which was comprised of only 16% *Salix spp.* and over 46% forb species. Another trend to note, with important implications to caribou population dynamics, is the low occurrence of lichen in all vegetative community types. Lichen ranged from 0% to 2% canopy cover across community types. These lichen species were almost exclusively in the foliose lichen group belonging to the *Peltigera* genus, a non-forage species of lichen, rather than the group of lichens belonging to the *Cladonia* genus, a key winter forage source of caribou.

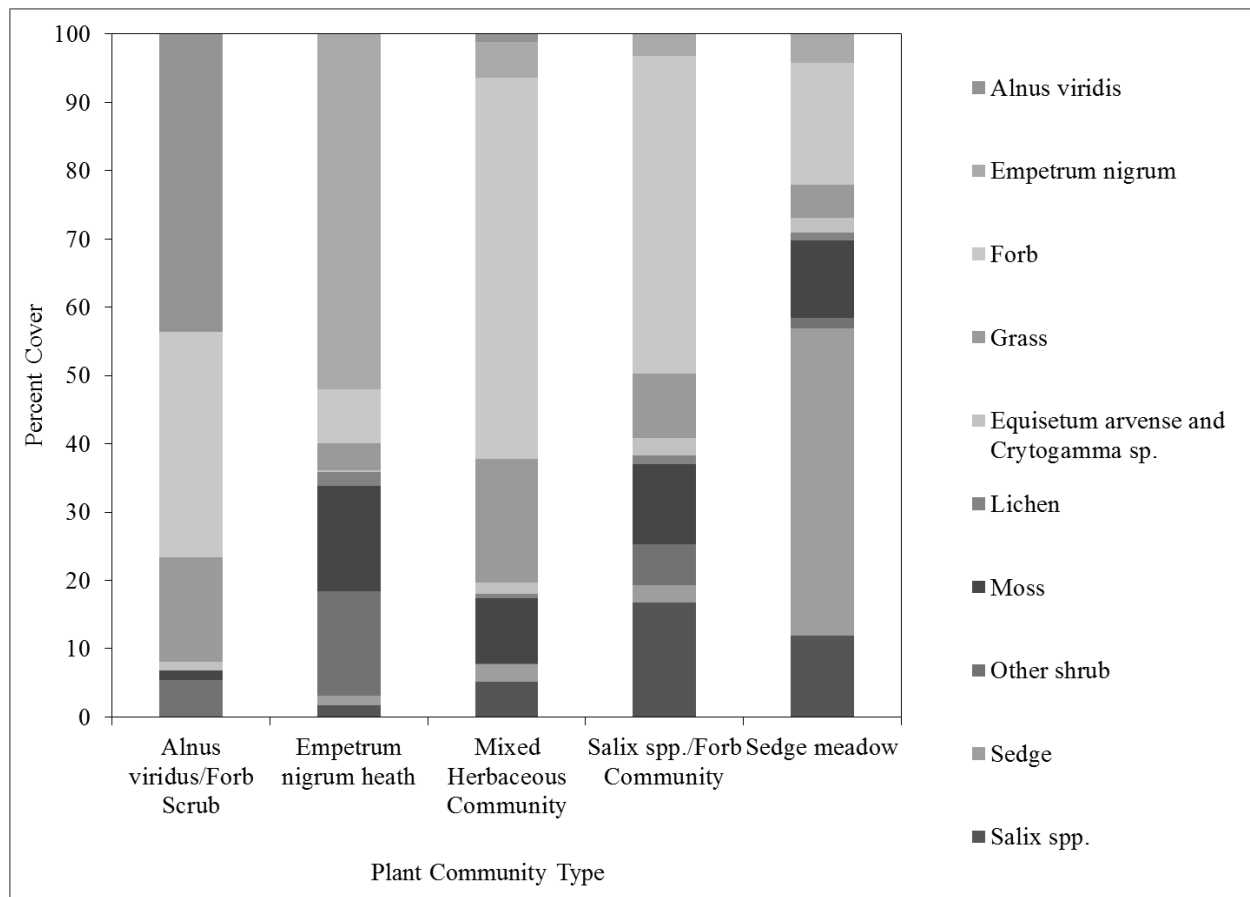


Figure 1.3 Canopy cover percentage by vegetative community type. Canopy cover was listed within each community type by plant functional group. *Empetrum nigrum* n=28, Sedge n=17, *Salix* spp./forb n=11, mixed herbaceous n=10, and *Alnus viridis*/forb n=4.

Accuracy Assessment

Two aerial photography transects located in the northeast side of Unimak Island were selected for the supervised classification accuracy assessment. These two transects were selected because of excellent overlap between all three dates of photography, and because they contained vegetation classes that represented all of the island’s vegetative communities. Approximately 12 photos were classified and assessed for accuracy for each photography date, covering an approximate land area of 0.40 km².

Summer aerial photography showed the greatest variability in spectral information for vegetative classes (Table 1.2, Figure 1.4). Spring aerial photography tended to have similar

spectral response patterns between deciduous plant types, such as willow and alder, and also between herbaceous plant types, such as sedge and mixed forb classes. Spectral response patterns in fall tended to be similar between willow and other vegetative plant groups. Alder was the most distinct from other plant groups during the fall date of aerial photography.

Table 1.2 Average, minimum and select pairwise transformed divergence values for vegetation classes.

Flight Date	Transformed Divergence Values					
	Average	Minimum	Willow:Alder	Willow:Sedge	Willow:Mixed Forb	Alder:Sedge
6/11/2011	1872	560	560	2000	1962	1999
7/3/2011	1920	1356	1966	2000	1938	1589
9/17/2011	1686	741	1472	1975	741	1618

Transformed divergence values for vegetation varied greatly by flight date (Table 1.2). Fall had the lowest values of transformed divergence, indicating poor separation, while summer had the highest transformed divergence value, indicating good separation. Spring had an intermediate value, indicating fair separation. Transformed divergence values also varied across dates between specific comparisons of vegetative classes (Table 1.2). Willow transformed divergence values appear to have the best separation during the summer, and fall transformed divergence values were low across many vegetative classes (Table 1.2).

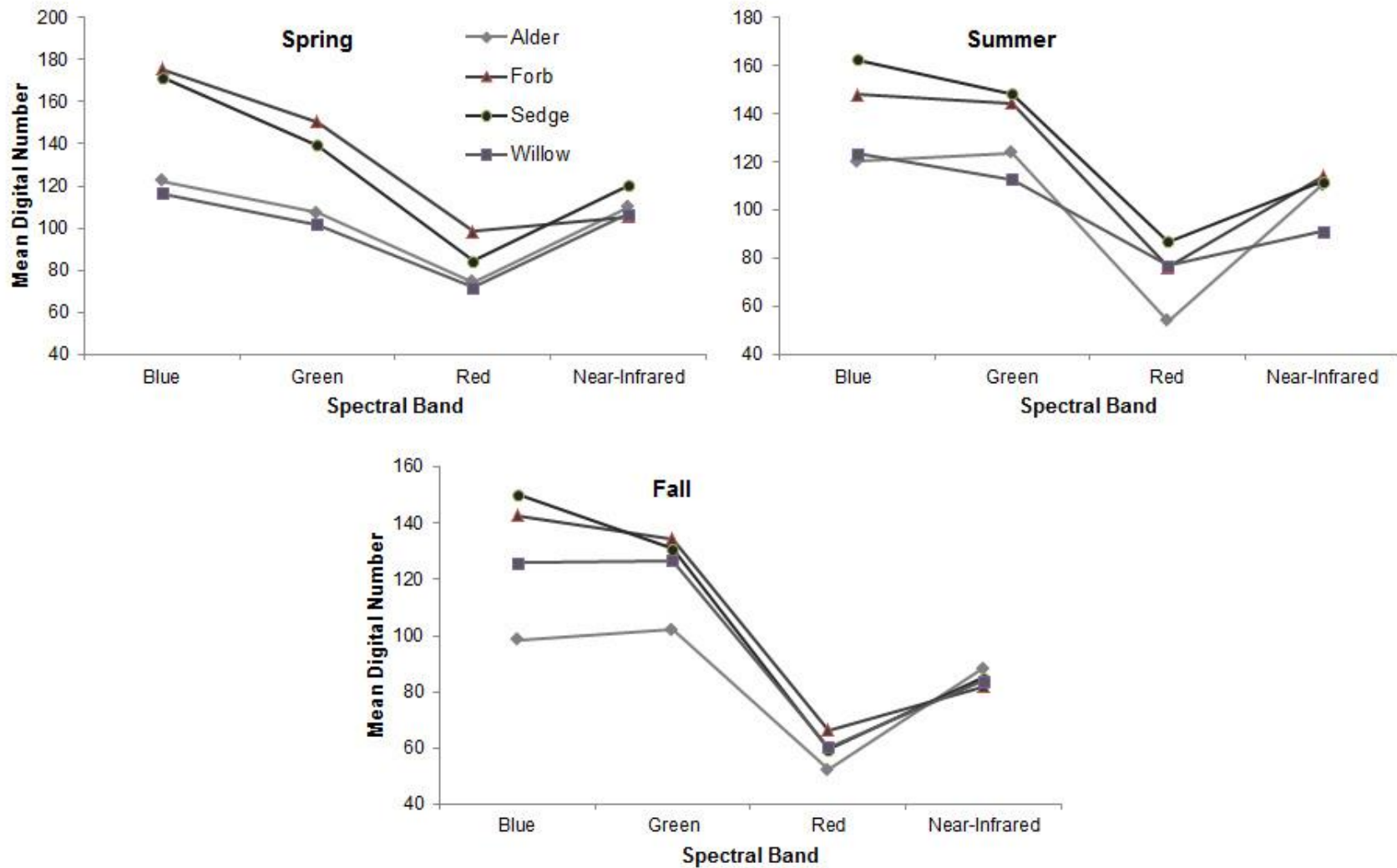


Figure 1.4 Spring, summer and fall comparisons of mean digital reflectance value by spectral band for select vegetation classes. Vegetation classes listed are alder, forb, sedge, and willow and spectral bands included are blue, green, red and near-infrared.

Average vegetative transformed divergence values by spectral band are listed in Table 1.3.

Spectral separability varies between bands and is dependent on date of imagery taken. For the spring date, the blue, green and red spectral information had the highest average spectral separability between vegetative classes, while the near-infrared had the lowest spectral separability.

Table 1.3 Average transformed divergence values by imagery acquisition date for vegetation classes.

Band	Average Transformed Divergence Values		
	6/11/2011	7/3/2011	9/17/2011
Blue	1846	1096	1752
Green	1841	1776	1430
Red	1742	1631	568
Near-infrared	817	1484	879

Overall and individual vegetation accuracy assessments were the highest for the summer (Table 1.4). Overall classification accuracy was the highest in summer (84%) and lowest for spring and fall classifications (78.1%). Classification accuracy dropped for all dates when calculated for vegetative classes only (Table 1.4). Spring classification had the lowest vegetation-only accuracy (72.3%), summer classification remained the highest accuracy (83.5%) with fall classifications having an intermediate accuracy rate (74.6%). Overall and vegetation-only kappa statistics were similar for the three dates of aerial photography when compared to classification accuracies. Kappa statistic values indicate that summer classification had the highest accuracy rate, followed by fall and spring dates of classification (Table 1.4).

Table 1.4 Overall and vegetation classification accuracies and Kappa statistic for 3 dates of aerial imagery acquisition. Imagery sample size: Spring n=10, Summer n=12, Fall n=10.

Flight Date	Overall Classification Accuracy	Vegetation Only Classification Accuracy	Overall Kappa Statistic	Veg-Only Kappa Statistic
6/11/2011	78.13	72.31	0.75	0.66
7/3/2011	83.98	83.51	0.81	0.79
9/17/2011	78.10	74.60	0.74	0.68

Producer's and user's accuracy assessments for sedge, willow, alder and mixed forb vegetative classes indicate that willow was selected most accurately during the summer (Table 1.5). The mixed herbaceous vegetative class remained relatively consistent through the three dates of aerial photography and classification, while alder increased sharply between spring and summer dates. Accuracy rates for sedge dropped following the spring acquisition. A visual comparison of maximum likelihood supervised classified images from all three dates of acquisition to a color-infrared image from fall are shown in Figure 1.5. Forb, alder and willow cover classes in the classified maps tended to increase in area through the summer.

Table 1.5 Producer's and user's accuracy for sedge, willow, alder and mixed forb communities.

Flight Date	Sedge		Willow		Alder		Mixed Forb	
	Producers	Users	Producers	Users	Producers	Users	Producers	Users
6/11/2011	85.7	90.0	53.6	57.7	63.6	60.9	69.8	61.2
7/3/2011	95.2	87.0	84.2	69.6	91.3	80.8	71.4	69.8
9/17/2011	78.3	72.0	51.5	50.0	88.9	88.9	77.1	69.1

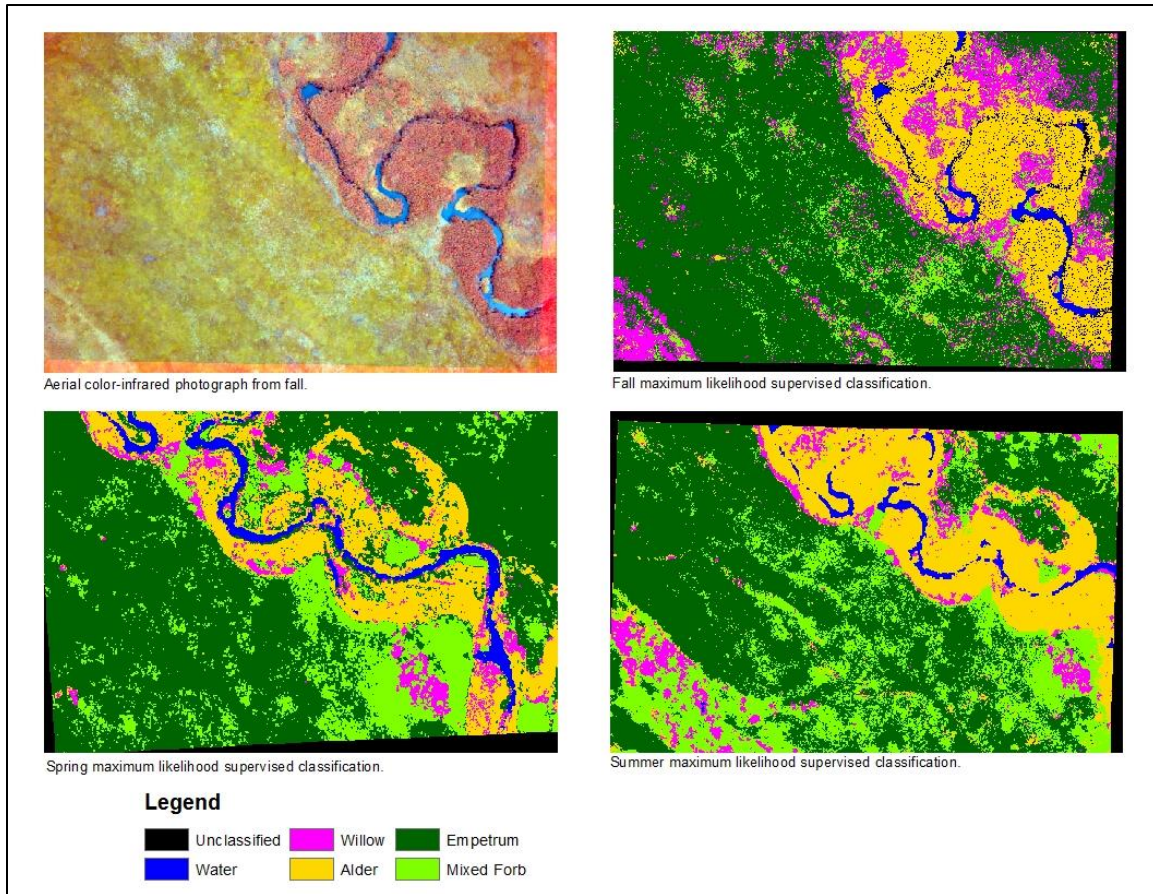


Figure 1.5 Maximum likelihood supervised classification from a single area from three dates of aerial imagery; spring, summer and fall.

DISCUSSION

High resolution color-infrared aerial photography is a means to develop highly accurate land cover maps for caribou management. Supervised classifications from low-level aerial photography proved to be highly accurate (~80% vegetation-only classification accuracy). Spring aerial imagery was the least accurate for vegetation-only classification and second most accurate for overall classification accuracy when compared to summer and fall dates. The decrease in accuracy between overall and vegetation only classification was due to the exclusion of accuracy assessment points from non-vegetated classes, such as riverbar and open water. These classes were significant in size and tended to raise the overall total correct number of accuracy assessment points. Summer photography and classification resulted in slightly higher vegetation-

only accuracy assessments compared to spring. Higher accuracy assessments for summer were the result of several vegetative communities, such as alder, having leafed out compared to early spring. All dates of aerial photography classifications were comparable to other low-level aerial land cover classifications in terms of classification accuracy (Walton et al., 2013). Summer classification accuracy was the highest for all dates of aerial photography, contradictory to our hypothesis that fall would produce the highest classification accuracy. Spring imagery tended to have confusion between vegetative classes because deciduous plant groups had not yet developed leaves and were in early bud development. Fall images had confusion and very low accuracy because all plant communities were leafed out, but the major differences in fall senescence had not yet occurred. Our fall date of acquisition may have been too early and plant senescence was missed, resulting in low spectral distinctness compared to the summer classification date. Satellite based remote sensing in the Northeastern United States has shown that forest vegetation is the most distinct during fall (Schriever & Congalton, 1995). Moose browse classifications from aerial photography were also found to be more accurate during the fall when spring and fall classifications were compared (Walton et al., 2013; Walton, 2009). Future research on Unimak Island and the Alaska Peninsula should expand the time frame for aerial photography to include a later date of imagery acquisition to assess whether a true senescence period would increase classification accuracy and to determine if the senescence period is long enough to use for classification purposes.

Future Research Areas

Low level aerial photography is a highly accurate means to develop land cover maps for caribou or large herbivore management. It is extremely useful for areas where landscape

heterogeneity may result in a complex landscape of mixed vegetative communities and remote sensing satellite platforms are unable to distinguish between these communities due to low spectral resolution. Future research should be directed at the feasibility and economics of large scale aerial photography acquisition and classification techniques for use in caribou and large herbivore management.

LITERATURE CITED

- Bartsch, A., Kumpula, T., Forbes, B. C., & Stammer, F. (2010). Detection of snow surface thawing and refreezing in the Eurasian Arctic with QuikSCAT: implications for reindeer herding. *Ecological Applications : A Publication of the Ecological Society of America*, 20(8), 2346–58.
- Cohen, W. B., & Goward, S. N. (2004). Landsat's Role in Ecological Applications of Remote Sensing. *BioScience*, 54(6), 535–545.
- Congalton, R. G. (1991). A Review of Assessing the Accuracy of Classifications of Remotely Sensed Data. *Remote Sensing of Environment*, 46, 35–46.
- Dale, B., Webber, M., Butler, L., Collins, W. B., Spalinger, D. E., Hundertmark, K., Martin, J., Watts, D., & Adams, L. G. (2013). *Population dynamics, genetics, and habitat characteristics of the Unimak Island Caribou Herd*.
- Daubenmire, R. (1959). A Canopy-Coverage Method of Vegetational Analysis. *Northwest Science*, 33(1), 43–64.
- Fancy, S. G., Pank, L. F., Whitten, K. R., & Regelin, W. L. (1989). Seasonal movements of caribou in arctic Alaska as determined by satellite. *Canadian Journal of Zoology*, 67(3), 644–650.
- Gordon, I. J., Hester, A. J., & Festa-Bianchet, M. (2004). REVIEW: The management of wild large herbivores to meet economic, conservation and environmental objectives. *Journal of Applied Ecology*, 41(6), 1021–1031.
- Hansen, M., Franklin, S., Woudsma, C., & Peterson, M. (2001). Caribou habitat mapping and fragmentation analysis using Landsat MSS, TM, and GIS data in the North Columbia Mountains, British Columbia, Canada. *Remote Sensing of Environment*, 77(1), 50–65.
- Heggberget, T. M., Gaare, E., & Ball, J. P. (2010). Reindeer (*Rangifer tarandus*) and climate change: importance of winter forage. *Rangifer*, 22(1), 13–31.
- Johnson, C. (2003). Characterizing woodland caribou habitat in sub-boreal and boreal forests. *Forest Ecology and Management*, 180(1-3), 241–248.
- Johnson, C. J., Parker, K. L., Heard, D. C., & Gillingham, M. P. (2002). Movement parameters of ungulates and scale-specific responses to the environment. *Journal of Animal Ecology*, 71(2), 225–235.
- Johnson, C., Parker, K., & Heard, D. (2001). Foraging across a variable landscape: behavioral decisions made by woodland caribou at multiple spatial scales. *Oecologia*, 127(4), 590–602.

- Kokaly, R. F., Asner, G. P., Ollinger, S. V., Martin, M. E., & Wessman, C. a. (2009). Characterizing canopy biochemistry from imaging spectroscopy and its application to ecosystem studies. *Remote Sensing of Environment*, 113, S78–S91.
- LDP LLC (2014) at <http://www.maxmax.com> (last accessed 25 June 2014)
- Mårell, A., & Edenius, L. (2006). Spatial heterogeneity and hierarchical feeding habitat selection by reindeer. *Arctic, Antarctic, and Alpine Research*, 38(3), 413–420.
- Post, E., & Forchhammer, M. C. (2008). Climate change reduces reproductive success of an Arctic herbivore through trophic mismatch. *Philosophical Transactions of the Royal Society of London. Series B, Biological Sciences*, 363(1501), 2369–75.
- Post, E., Pedersen, C., Wilmers, C. C., & Forchhammer, M. C. (2008). Warming, plant phenology and the spatial dimension of trophic mismatch for large herbivores. *Proceedings. Biological Sciences / The Royal Society*, 275(1646), 2005–13.
- Schriever, J. R., & Congalton, R. G. (1995). Evaluating Season Variability as an Aid to Cover-Type Mapping from Landsat Thematic Mapper Data in the Northeast. *Photogrammetric Engineering and Remote Sensing*, 61(3), 321–327.
- Shipley, L. A., & Spalinger, D. E. (1992). Mechanics of browsing in dense food patches: effects of plant and animal morphology on intake rate. *Canadian Journal of Zoology*, 70(9), 1743–1752.
- Stien, A., Loe, L. E., Mysterud, A., Severinsen, T., Kohler, J., & Langvatn, R. (2010). Icing events trigger range displacement in a high-arctic ungulate. *Ecology*, 91(3), 915–20.
- Story, M., & Congalton, R.G. 1986. Accuracy assessment: a user's perspective. *Photogrammetric Engineering and Remote Sensing*. 52: 397-399.
- Talbot, S. S., Talbot, S. L., & Schofield, W. B. (2006, October). Vascular flora of Izembek National Wildlife Refuge, Westernmost Alaska Peninsula, Alaska. *Rhodora*.
- Théau, J., Peddle, D. R., & Duguay, C. R. (2005). Mapping lichen in a caribou habitat of Northern Quebec, Canada, using an enhancement-classification method and spectral mixture analysis. *Remote Sensing of Environment*, 94(2), 232–243.
- Trudell, J., & White, R. G. (1981). The Effect of Forage Structure and Availability on Food Intake , Biting Rate , Bite Size and Daily Eating Time of Reindeer. *Journal of Applied Ecology*, 18(1), 63–81.
- Tyler, N. J. C. (2010). Climate, snow, ice, crashes, and declines in populations of reindeer and caribou (*Rangifer tarandus* L.). *Ecological Monographs*, 80(2), 197–219.

- U.S. Fish and Wildlife Service. (2010). *Management Alternatives for the Unimak Island Caribou Herd: Environmental Assessment* (pp. 1–94).
- Ustin, S. L., Gitelson, A. A., Jacquemoud, S., Schaepman, M., Asner, G. P., Gamon, J. A., & Zarco-Tejada, P. (2009). Retrieval of foliar information about plant pigment systems from high resolution spectroscopy. *Remote Sensing of Environment*, 113, S67–S77.
- Viereck, L. A., Dyrness, C. T., & Batten, A. R. (1992). *The Alaska Vegetation Classification*.
- Vors, L. S., & Boyce, M. S. (2009). Global declines of caribou and reindeer. *Global Change Biology*, 15(11), 2626–2633.
- Walton, K. M. 2009. Landscape scale quantification of wildlife habitat using hierarchical classification techniques. Thesis. University of Alaska Anchorage, Anchorage, USA.
- Walton, K., Spalinger, D. E., Harris, N. R., Collins, W. B., & Willacker, J. J. (2011). Landscape Scale Quantification of Wildlife Habitat using Landsat Imagery and Hierarchical Classification Techniques. *Submitted*.
- Walton, K. M., Spalinger, D. E., Harris, N. R., Collins, W. B. and Willacker, J. J. (2013), High spatial resolution vegetation mapping for assessment of wildlife habitat. *Wildlife Society Bulletin*, 37: 906–915.
- White, R.G. 1983. Foraging patterns and their multiplier effects on productivity of northern ungulates. *Oikos* 40(3):377-384.
- White, R.G. and J. Trudell. 1980. Habitat Preference and Forage Consumption by Reindeer and Caribou near Atkasook, Alaska. *Arctic and Alpine Research* 12(4):511-529.
- Wilson, F.H., Miller, T.P., and Detterman, R.L. (1992). Preliminary geologic map of the Cold Bay and False Pass quadrangles, Alaska Peninsula: U.S. Geological Survey Open-File Report 92-545, 10 p., 1 sheet, scale 1:250,000.
- Wilson, R., Bartsch, A., Joly, K., Reynolds, J., Orlando, A., & Loya, W. (2013). Frequency, timing, extent, and size of winter thaw-refreeze events in Alaska 2001–2008 detected by remotely sensed microwave backscatter data. *Polar Biology*, 36(3):419-426.
- Xie, Y., Sha, Z., & Yu, M. (2008). Remote sensing imagery in vegetation mapping: a review. *Journal of Plant Ecology*, 1(1), 9–23.

CHAPTER 2: HIGH RESOLUTION SATELLITE IMAGERY TO QUANTIFY AND DELINEATE CARIBOU HABITAT ON UNIMAK ISLAND₂

ABSTRACT

In this study we acquired remotely sensed imagery from the multi-spectral satellite imagery company Rapideye. By using RapidEye and aerial digital imagery in a hierarchical supervised classification technique, we were able to produce a highly accurate land cover map of Unimak Island. Aerial imagery for development of large herbivore habitat maps provides a fine scale assessment of vegetative cover. While this method can provide high resolution land cover information, it may not be the most efficient means to obtain landscape scale maps, as large herbivores generally occupy very large home ranges. Previously developed land cover maps are generally produced at a resolution in which small but important forage communities, such as willow, cannot be identified. The Unimak Island caribou herd has been decreasing in the last decade at rates that have prompted discussion of management intervention. The extreme remoteness of our study area has provided for little opportunity or knowledge of the caribou forage habitat or the caribou herd population dynamics on Unimak Island. Furthermore, frequent and persistent cloud cover over Unimak Island and the Alaska Peninsula has made the acquisition of remote sensing imagery difficult. We obtained overall accuracy rates of 71.5% which is comparable to other land cover maps produced using RapidEye imagery. Several composite images were constructed to assess the importance of the “red-edge” spectral band. We found that the “red-edge” spectral band provided important spectral information that allows for a more accurate overall classification. We also found that the RapidEye classification had a much

higher accuracy, 74.1%, when it was standardized and compared to the accuracy of land cover classes in the National Land Cover Dataset (NLCD), 39.7%.

INTRODUCTION

Decline of Caribou

Caribou (*Rangifer tarandus*) populations have been declining throughout the world (Vors & Boyce, 2009) at a rate that has prompted concerns about population longevity. These trends of population decline have also been observed for many caribou herds throughout Alaska (Valkenburg et al., 2003, U.S. Fish and Wildlife Service 2010). The Unimak Island caribou herd in southwest Alaska is one such herd, and its continued sharp decline over the past decade has prompted discussion of drastic intervention in an attempt to prevent the extinction of this population (U.S. Fish and Wildlife Service 2010).

While wolves and brown bears are known to predate on calves on Unimak Island, and have limited calf recruitment in other nearby herds on the Southern Alaska Peninsula (Dale et al., 2013; U.S. Fish and Wildlife Service, 2010), the role of forage quality and quantity on the Unimak Island caribou herd is not understood. Forage quality is related to the multiple factors, but for large herbivores generally includes whether the forage protein content and the digestibility of the forage are adequate to sustain population growth or individual physiologic processes. Many environmental factors, particularly weather and climate related, greatly influence the growth of forage plants and their subsequent quality, through direct and indirect effects. Due to the trends of circumpolar decline of caribou herds, several global climate change/forage quality relationships have been proposed that may influence caribou population dynamics. These include the increased occurrence of freeze-thaw cycles that lock vital winter forage under layers of ice (Heggberget et al., 2010; Stien et al., 2010; Tyler, 2010), and also a process termed trophic mismatch (Post & Forchhammer, 2008; Post et al., 2008). In order to

evaluate the quality of caribou habitat and potential climate change effects on caribou habitat, an assessment of the spatial distribution of forage species is required.

Land Cover Determination

The management of large herbivores generally requires an accurate assessment of the forages that are available to that herbivore, both spatially and temporally (Mårell & Edenius, 2006). In order to assess habitat quality, an estimate of available forage and quality is needed (Trudell & White, 1981). Traditionally, this was accomplished through the use of hand clip plots to estimate forage biomass and nutritional quality. Estimating the available forage can be difficult because of the large area that an animal can occupy as its habitat. This is especially true for migratory animals such as caribou (*Rangifer tarandus*) that can migrate thousands of kilometers annually and have a home range of thousands of square kilometers (Fancy et al., 1989). Remote sensing and the use of land cover maps have become an important tool for land managers wishing to determine the distribution of forage plants for large herbivores. A land cover map can provide the basic spatial coverage and distribution of vegetative communities over a very large area. This map can be coupled with biomass estimates to give an approximate idea of forage production, and with nutritional information to provide a habitat quality assessment.

Remote sensing through the use of various detectors of electromagnetic energy has proven to be an efficient and effective means of quantifying vegetative traits across vast landscapes. The advancement of remote sensing techniques over the last two decades has allowed for the detection of a variety of canopy biochemistry characteristics (Kokaly et al., 2009; Ustin et al., 2009), and increased accuracy of classification of vegetation communities (Xie et al.,

2008). Remote sensing has been widely adapted for use in ecology and has proven to be very useful in large-area mapping and assessment of habitat (Cohen & Goward, 2004).

The spatial distribution of forage is an important aspect for habitat assessment and management of large herbivores (Gordon et al., 2004). Unfortunately, this can prove difficult to evaluate because of the hierarchal scale of foraging; areas that herbivores utilize can range from small foraging sites of a single forage species, up to large heterogeneous plant community landscapes composed of many individual vegetative communities (Johnson et al., 2002; Johnson et al., 2001; Shipley & Spalinger, 1992) The use of remote sensing techniques addresses this issue by allowing for a plant community resolution with landscape scale coverage. There are many examples of the use of remote sensing for evaluating caribou habitat. Johnson (2003) successfully mapped 27 vegetation types across boreal and sub-boreal caribou habitat in northcentral British Columbia, Canada using Landsat TM imagery and ancillary GIS data. Théau et al. (2005) also used Landsat TM imagery and two classification methods to map lichen abundance, an important winter forage of caribou, in northern Quebec, Canada. Hansen et al. (2001) utilized both Landsat MSS and Landsat TM imagery to evaluate land cover change and habitat fragmentation for mountain caribou habitat range in British Columbia, Canada. Finally, Bartsch et al. (2010) was able to correlate observed rain-on-snow events and the subsequent formation of ice layers on caribou winter range using backscatter data from the QuikSCAT scatterometer. Clearly, remote sensing has many uses in caribou habitat assessment, largely due to the fact that migrating herds occupy vast landscapes and remote sensing allows for effective evaluation and monitoring of the habitat. Unfortunately, remote sensing data usually are not detailed enough at the ground level to distinguish fine differences in habitat types, due to the low spatial resolution of the imagery. Current widespread imagery typically used for land cover maps

is from the Landsat program. This spectral data has a spatial resolution of 30 meters on a side. While this can allow for broad community type classifications, it often fails to detect vegetation communities of a smaller size that are often of high nutritional importance.

While this Landsat imagery is available for Unimak Island, it is limited seasonally by the high cloud cover over the Aleutian Islands and the Southern Alaska Peninsula. Due to this and the extreme weather and remoteness of the area, little is known about this herd or its habitat (Valkenburg et al., 2003). In order to address the lack of caribou forage and vegetation distribution knowledge on Unimak Island, we propose to develop and assess remote sensing techniques to produce a land cover map using high-resolution satellite imagery from RapidEye imagery and aerial photography. The objectives of this chapter were four-fold: 1) to map the distribution of caribou forage on Unimak Island for wildlife management purposes; 2) to assess the use of RapidEye in landscape-wide vegetation classification; 3) to determine if the inclusion of a “red-edge” spectral band significantly increases the classification accuracy of satellite imagery vegetation classification; and 4) to compare the classification accuracy and class assignments of the National Land Cover Database classification map, (NLCD), to that of a Rapideye land cover classification map.

METHODS

Study Site Description

Unimak Island (Figure 2.1) (54.7683° N, -164.1867° W) is a volcanic island that lies at the easternmost end of the Aleutian Island Archipelago in southwestern Alaska. Its land area is approximately 4,000 km² and is the largest of the 69 Aleutian Islands. It is separated from the southern tip of the Alaska Peninsula by the narrow Isanotski Strait, which is approximately 700

meters wide. This narrow strait has allowed for populations of caribou (*Rangifer tarandus*), brown bear (*Ursus arctos*), wolf (*Canis lupis*), and red fox (*Vulpes vulpes*) to occasionally cross to the island. Hence, it is the only Aleutian Island with naturally occurring populations of these fauna (U.S. Fish and Wildlife Service, 2010). Unimak Island (Figure 2.1) is classified as a marine tundra environment and is characterized by the absence of trees, large areas of barren ground from geologically-recent volcanic activity and high winds, and a sharp increase in elevation, from sea level to 2,857 meters (Mount Shishaldin), in just over 14 km.

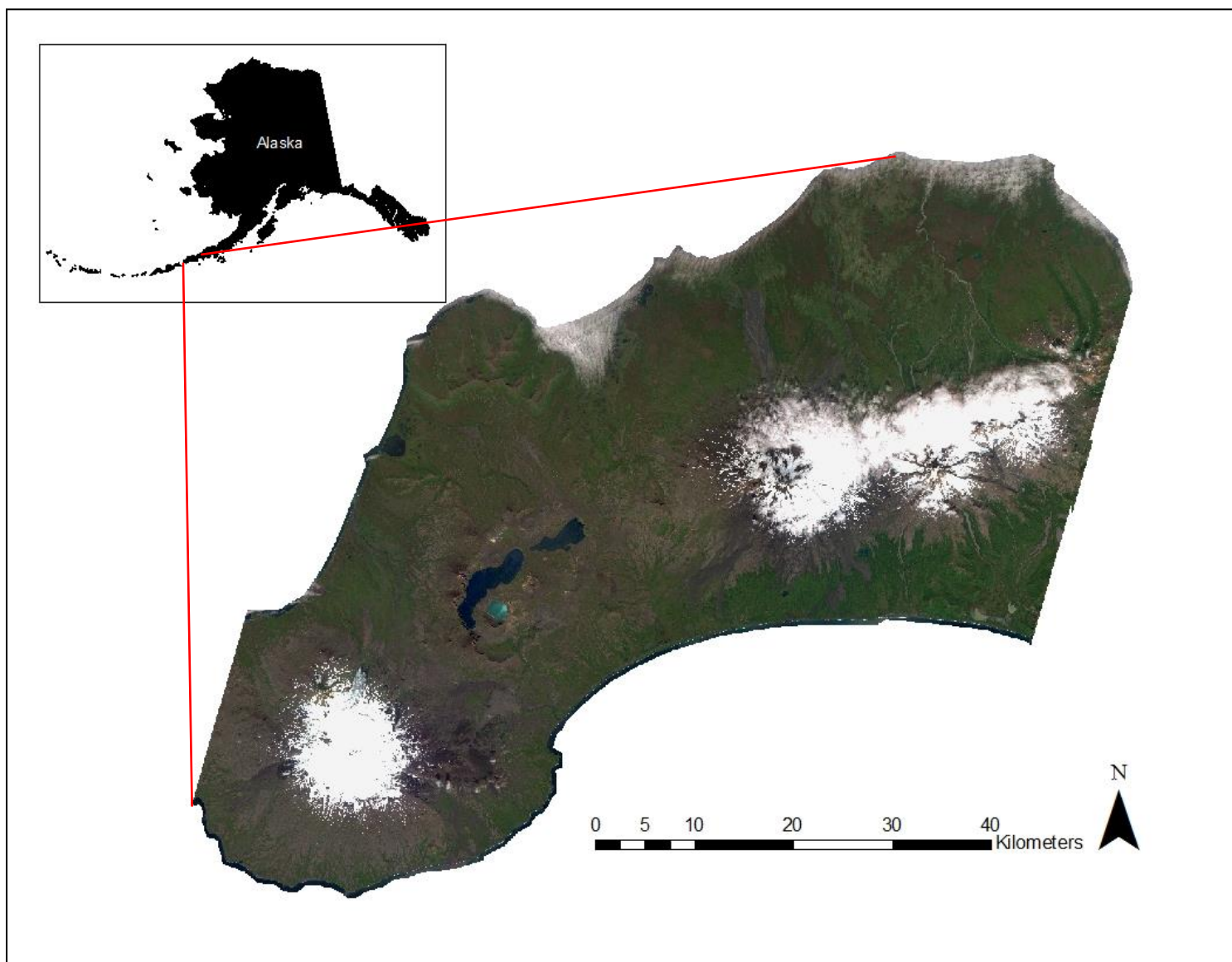


Figure 2.1 RapidEye color image of a subset of Unimak Island. Taken on August 12th 2011. The upper-left sub-graphic shows a reference image of Alaska, and indicates the geographic location of Unimak Island with respect to Alaska.

Dominant vegetation species across the island include dwarf-shrub crowberry (*Empetrum nigrum*), sedge (*Carex spp.*), alder (*Alnus crispa*), willow (*Salix spp.*), and other herbaceous forb species (Talbot et al., 2006). Vegetative community cover types followed a modified Viereck Alaska Vegetation Classification system (Viereck et al., 1992). Each vegetative community was assigned to a level IV classification. Classes following this system included low-scrub willow, tall shrub alder, herbaceous graminoid – wet (emergent wetlands), herbaceous forb communities, and dwarf scrub empetrum tundra. For the purposes of our classification, a dominant vegetation class is defined as a plant community where greater than 50% of the species present on an area basis are of one plant species. This distinction allows for a broader classification of vegetation species into vegetative community types. While we evaluated the entire island and all of its vegetative community types, caribou are known to only forage on a few species found on Unimak Island. These forage types generally consist of forbs, grasses and sedges, and shrubs within the genus *Salix* (White, 1983; White and Trudell, 1980). Caribou are not known to forage on other shrub species that occur on Unimak Island, such as *Alnus viridis*, *Arctostaphylos uva-ursi*, *Empetrum nigrum*, *Vaccinium uliginosum*, and *V. vitis-idaea*. Lichen species are a major component of caribou winter diet, mainly consisting of lichens in the *Cladonia* genus. Lichen species that were found were mainly in the *Peltigera* genus, a non-forage species of caribou. No lichen communities were established for this study on Unimak Island.

Vegetation classes identified in RapidEye imagery were similar to those identified in the aerial imagery classification of Unimak Island from Chapter 1. The dwarf scrub empetrum tundra class was split into a “live” and a “dead” class due to the high spatial occurrence of non-photosynthetically active *Empetrum nigrum* plants. Vegetative classes identified in the RapidEye

classification will hereafter be simply referred to as willow, alder, sedge, mixed forb, empetrum, and empetrum-dead. Non-vegetative land cover classes in the RapidEye land cover map included open water, snow/ice cover, cloud cover, and barren ground.

Satellite Imagery

Persistent and frequent cloud cover over Unimak Island and the Alaskan Peninsula resulted in very few usable satellite images available for use in developing a land cover map. The Landsat archive, dating from 1972, only has three images with less than 20% cloud cover for Unimak Island. Additionally, the failure of the scan line corrector on the Landsat 7 Enhanced Thematic Mapper Plus (ETM+) satellite in May 2003, left many images with large gaps in data (Markham et al, 2004). Landsat 5 Thematic Mapper (TM) provided one cloud-free image of Unimak Island on May 2006, but this image was taken shortly after the winter period and spectral differences in vegetation were subdued.

Level 3A orthorectified satellite imagery was obtained for Unimak Island from RapidEye[®], a German-based remotely-sensed imagery acquisition company. The imagery was acquired on August 13th, 2011. The spatial resolution of the sensor is 5 meters on a side and the extent of the image covers approximately 90% of the entire island. The field of view (FOV) of the RapidEye sensor allows for a 77 km swath width at nadir, whereas Unimak Island is approximately 120 km wide in the east-west orientation. The RapidEye sensor collects 5 wavelengths of spectral information. The spectral range of the wavelengths of the bands in nanometers are as follows: Blue: 440 - 510; Green: 520 - 590; Red: 630 - 685; Red Edge: 690 - 730; and Near-infrared (NIR): 760 - 850.

Training Sites/Ground Truthing

Spot samples of vegetation spectral response patterns across the island were obtained using high resolution aerial digital photography, as outlined in the methods of chapter 1. Methods for obtaining and classifying aerial imagery followed that of Walton et al. (2011, 2013). High resolution digital images were taken along 55 single-line transects in areas with anecdotal evidence of high densities of caribou. These areas were mainly along the north-eastern side of the island as this was where caribou were often spotted on previous aerial surveys of the herd (William Collins, personal communication). Transects were also taken along the western and southern side of the island but the majority of ground-truthing of aerial imagery occurred in the north-eastern area of the island because of logistical constraints. Aerial images were taken during three phenologically distinct periods of plant growth. These periods included green-up in early spring, peak-growth in mid-summer and during senescence in the fall. Each transect consisted of 20-25 photographs covering a distance of approximately 3 km. Color images were taken with a Canon EOS Rebel T2i 18.0 Megapixel camera with an EF-S 18mm lens with a UV filter. Near-infrared images were taken with the same model camera modified for capturing infrared (LDP LLC, 2014) outfitted with the same lens and a Tiffen[®] 85C infrared filter. Infrared and color images were taken at an altitude of approximately 150 meters through the belly port of a Found Bush Hawk XP fixed-wing plane in 2011 and from the strut of a R44 helicopter in 2012. Images taken at this altitude cover an area approximately 185 by 125 meters with a resolution of 3.5 cm on a side.

Ground-Truthing

Selected aerial photographs from the beginning, middle, and end point of each transect were ground-truthed using a Trimble® Pathfinder Pro XRTM backpack GPS unit or a Trimble® Geo XT handheld GPS unit. The selection of images that were ground-truthed was based on feasibility of getting to photographed locations, and to maximize and capture variability of vegetative cover types across the island. Ground control points (GCPs) were selected based on features across the photos that were recognizable on the ground. 15 - 30 GCPs were selected per image for the initial orthorectification. GCPs were real-time corrected to the nearest base station and the majority of points had sub-meter accuracy. Points collected with the Pathfinder Pro XR GPS unit had an average horizontal accuracy of 0.4 meters and points collected with the Geo XT GPS unit had an average horizontal accuracy of 0.8 meters. Images were orthorectified in the ERDAS Imagine® LPS Project Manager using the collected GCPs, an ASTER digital elevation model (24 meter spatial resolution) of Unimak Island, and a Canon T2i camera model. All images were resampled using a nearest neighborhood resampling method resulting in spatial accuracies of less than 2 meters. Images were then mosaicked using the MosaicPro tool in ERDAS Imagine® if overlapping orthorectified images were available.

Orthorectified aerial images had sub-meter accuracy and were assumed to be highly accurate relative to the RapidEye imagery. When orthorectified aerial images were overlaid on the RapidEye satellite imagery, the RapidEye tiles appeared to be shifted relative to the higher resolution aerial photography, sometimes resulting in a spatial error of 30 or more meters. Locational accuracy assessments for Level 3A ortho RapidEye imagery is 50 meter CE90 or 32 meter RMSE. Our visual assessment of RapidEye spatial accuracy relative to the aerial imagery was approximately within this spatial accuracy assessment. In order to correct for this source of

spatial error, each orthorectified image was shifted to best match features identifiable in the RapidEye satellite image, such as rivers, barren ground and vegetation transition areas.

Individual aerial images were shifted rather than the RapidEye image being shifted, because the amount of spatial displacement varied between each set of aerial images. In order to correct for the shift of aerial imagery relative to RapidEye, each aerial image was adjusted by altering the upper left x and y coordinates of the aerial imagery metadata. This is a translational shift and assumes a flat topography. The goodness of fit to the satellite image was assessed visually and appeared to be less than 1 RapidEye pixel in most areas.

Unsupervised and Supervised Classification Methods

Land cover classes for the RapidEye satellite image were similar to cover classes previously used in the aerial imagery classifications. Training sites were established in, and spectral information was extracted from the following classes: barren ground, cloud cover, permanent ice/snow, open water, empetrum, empetrum - dead, herbaceous forb, sedge, willow, and alder. Vegetative and non-vegetative training sites were digitized either directly from the RapidEye image, or from the orthorectified aerial images. A minimum of 20 training sites were selected for each class, with an emphasis to include areas from across the entire island to capture variability of spectral information. Extracted RapidEye spectral data was then used as the class parameters in the maximum likelihood classification.

Transformed divergence values were also created to give an estimate of the separability of the land classes using the spectral information from the satellite. Values are unit-less and range from 0 – 2000. Jensen's (1996) general rule of transformed divergence values was used to group values into categories. Values of 1900 and above indicate good separation between

trainings groups. Values between 1700 and 1900 indicate moderately well separated values, and values below 1700 indicate poor separation. Spectral response patterns, transformed divergence values and visual inspection of each classified image were used to assess the initial selection of training sites.

Accuracy Assessment

To assess the accuracy of the classification map created, a cross-tabulation method was used similar to the accuracy assessment of the aerial imagery classifications in Chapter 1. A stratified random sampling scheme was used to create reference points within the aerial imagery. A minimum of 20 random points per land cover class, resulting in a total of 320 points, were selected within the orthorectified aerial images that were not used in training site selection. This allowed for a more valid accuracy assessment because the resulting cross-tabulation is not based on spectral data that was used in the classification algorithm.

To assess classification accuracy of the RapidEye land classification map, overall accuracy, Producer's accuracy and User's accuracy were calculated. User's accuracy reports the probability of a pixel produced in the classified map actually being located on the ground. Producer's accuracy reports the probability of a referenced pixel to be correctly mapped (Story and Congalton, 1986). Kappa statistics were also produced, an assessment of accuracy that takes into account the agreement of classification due to chance (Congalton, 1991).

Red-edge Spectral Band Assessment

The red-edge band of spectral information is a relatively new commercially available remote sensing spectral band. It is generally identified as the region of the electromagnetic

spectrum from 680 nm to 730nm. This region is the area of the electromagnetic spectrum that increases rapidly in vegetative reflectance between the red and near-infrared bands. Reflectance of visible red light is low because of energy conversion through photosynthesis while the reflectance of near-infrared from vegetation is strong (Jensen, 1996). RapidEye is one of the first commercial satellites to provide the red-edge band for spectral information. RapidEye's red-edge band has been shown to increase the detection of stressed vegetation (Eitel et al., 2011) and the inclusion of the red-edge band with RapidEye imagery has also been shown to increase the accuracy of land cover classifications (Schuster et al., 2012). In order to test the effectiveness of inclusion of the red-edge band on the classification accuracy of caribou forage habitat on Unimak Island, several classifications were performed using RapidEye composite images. A composite image was produced by subtracting the red-edge band from the original 5-band RapidEye image, creating a 4-band image, which will be referred to as the RapidEye – RE image. This composite image allowed for a direct comparison to assess whether the red-edge spectral information increases classification accuracy.

A normalized difference vegetative index (NDVI) image was produced from the red and near-infrared bands in ERDAS Imagine[®]. This spectral band was used to create a second set of composite images (Schuster et al., 2012). The second composite image was created by replacing the red-edge band with an NDVI band, which allows for a comparison of whether replacement spectral information in substitution of the red-edge information can produce an equally high accuracy assessment. This composite image will be referred to as the RapidEye – RE + NDVI image. A third composite image was created by adding the NDVI band to the original RapidEye image. This was done to assess if an increase or decrease in accuracy with the RapidEye - RE + NDVI image was due to the addition of the NDVI band or due to the replacement of the red-edge

band. This composite image will be referred to as the RapidEye + NDVI image. RapidEye composite images are listed in Table 2.1.

Table 2.1 List of RapidEye composite images used to assess the red-edge band.

RapidEye Composite Image	Description	Number of Bands
RapidEye	Original RapidEye image	5
RapidEye - RE	Original RapidEye image minus the Red-Edge band	4
RapidEye + NDVI	Original RapidEye Image plus an NDVI spectral band	6
RapidEye - RE + NDVI	Original RapidEye image minus the Red-Edge band, plus an NDVI spectral band	5

Maximum likelihood supervised classifications were then performed on the three RapidEye composite images by selecting and extracting the spectral information from the training sites developed for the original RapidEye classification. Accuracy assessments were performed on the composite images by adjusting and using the same set of original stratified random reference points in order to have the most direct comparison between classified composite images. Transformed divergence values were also calculated for each RapidEye composite image to assess the spectral separability between images and individual spectral bands. Transformed divergence values were also used to assess whether the inclusion of the red-edge band provided beneficial spectral information relative to the other RapidEye composite images.

Comparison to NLCD

An accuracy assessment was run for one of the few land cover maps of Unimak Island, the National Land Cover Database (NLCD) for comparison to the original 5-band RapidEye classification map. The NLCD is a nationally produced land cover map of the entire United States and is produced by The Multi-Resolution Land Characteristics Consortium (MRLC) (Fry et al., 2011). This vegetation classification map was based on a Landsat 5 TM (Thematic Mapper) image from May 2006. This particular Landsat image is the only Landsat image with

adequately low cloud cover to produce a vegetation classification map of the entire island. Vegetative classes were combined in the RapidEye land cover classification to match the NLCD classes to allow for a direct comparison between RapidEye and NLCD. The vegetative classes of the NLCD include the following: Shrub/Scrub, Dwarf Shrub, Grassland Herbaceous, Woody Wetlands and Emergent Herbaceous Wetlands. Empetrum and empetrum - dead classes were combined in the RapidEye land cover image to create the Dwarf Shrub class; the willow and alder classes were combined to create the Shrub/Scrub class. The sedge class was substituted directly for Emergent Herbaceous Wetlands class of NLCD, and the mixed herbaceous forb class was substituted directly for the Grassland/Herbaceous class. The accuracy assessment was created for the NLCD by using the same 320 random reference points that were used in the original RapidEye accuracy assessment.

RESULTS

The total area from the RapidEye classification was 380,898 hectares (ha), approximately 93% of the total land area of Unimak Island (Table 2.2). Non-vegetative classes compromised 42.3% of the areal coverage including cloud cover. The empetrum class accounted for the highest areal coverage of all classes at 91,219 ha or 23.9 % of the total land cover. Empetrum and empetrum - dead classes together made up 36.4 % of the total area coverage or 138,695 ha. All other vegetative classes were relatively small compared to the empetrum class. The next highest coverage compared to the empetrum classes was the sedge class at 34,619 ha or 9.1 %. The smallest coverage was for alder at 12,038 ha or 3.2 % of the total land cover (Table 2.2).

Table 2.2 Areal coverage of land cover classes in hectares from the RapidEye maximum likelihood classification.

Class Name	Area - Hectares	Percent Coverage	Vegetation Percent Coverage
Open Water	12,403	3.3	--
Snow/Ice	17,028	4.5	--
Cloud Cover	51,802	13.6	--
Barren Ground	79,533	20.9	--
Empetrum	91,219	23.9	41.4
Empetrum - Dead	47,476	12.5	21.6
Willow	15,733	4.1	7.1
Alder	12,038	3.2	5.5
Mixed Herbaceous Forb	19,047	5.0	8.7
Sedge	34,619	9.1	15.7
Total	380,898	100	100

Several spatial patterns of land cover were observed, as can be seen in Figure 2.2. Cloud cover was concentrated around high elevations and along the northern edge of the Unimak Island/Bering Sea coastline. Permanent snow and ice were concentrated around the higher elevation glacier-clad areas associated with volcanoes. Barren ground was found around higher elevation areas, river corridors and on the southwestern end of Unimak Island. These areas are associated with disturbance through volcanic or glacier activity, exposure to high wind, or flood prone areas in riparian corridors. Sedge or wet herbaceous graminoid communities were mainly found in low elevation, tidally influenced areas close to the coastline. Empetrum classes were extensive on the northern side of Unimak Island, while alder was more likely to be found on the southeastern end of Unimak Island. Willow, alder, and mixed herbaceous forb communities were found across the island and were mostly associated with riparian and disturbance areas.

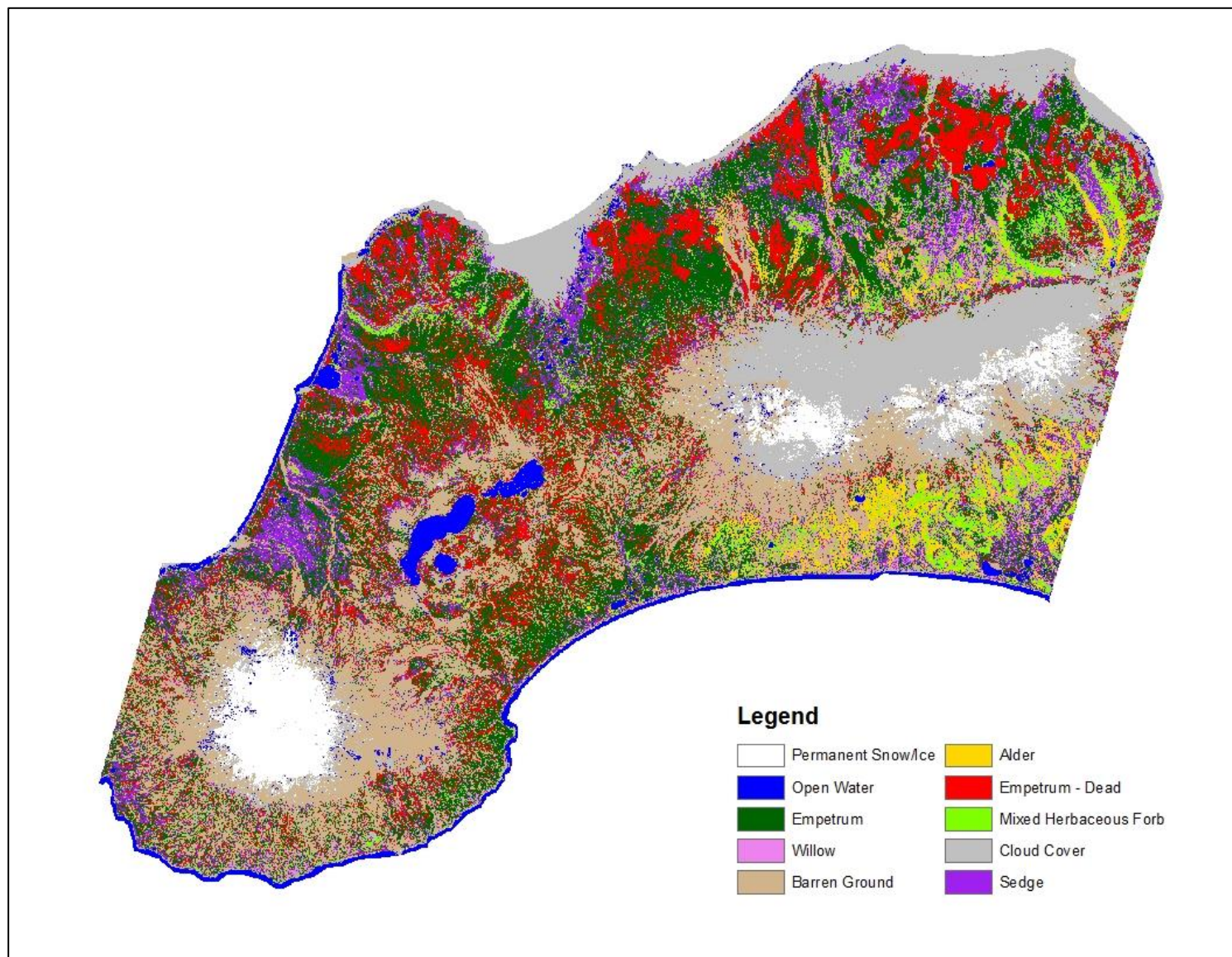


Figure 2.2 RapidEye maximum likelihood classification image of Unimak Island.

Accuracy Assessment

The overall accuracy rate for the RapidEye classification image was 71.56% (Table 2.3), which was similar to, but slightly lower than the accuracy of comparable land cover maps produced using RapidEye; Schuster et al., 2012 (77.3%); Tapsall et al., 2010 (81%); Tigges et al., 2013 (85.5%). Overall kappa statistic value for the RapidEye classification was 0.66, indicating lower accuracy based on chance agreement between classes.

Table 2.3 Overall accuracy and kappa statistic for the RapidEye maximum likelihood classification.

	Overall Classification Accuracy (%)	Overall Kappa Statistic
RapidEye Classification	71.56	0.66

Producer and user's accuracy rates by vegetation class ranged from 53.9% to 97.7% (Table 2.4). Kappa statistics ranged from a minimum of 0.46 for the mixed herbaceous forb class; to a maximum of 0.92 for the alder class (Table 2.4). Producer's accuracy was higher than the user's accuracy for the willow, empetrum - dead, and the mixed forb classes. User's accuracy rate was higher than the producer's accuracy for the sedge class, while the empetrum and alder classes had equivalent values for both producer's and user's accuracy rates. A higher user's accuracy relative to the producer's accuracy indicates that that particular class is being overestimated in the map, while a higher producer's accuracy relative to the user's accuracy indicates that that particular class is underestimated in the classification.

Table 2.4 Producer's accuracy, user's accuracy, and kappa statistic for vegetative community types.

Cover Class	Producers Accuracy	Users Accuracy	Kappa Statistic
Empetrum	76.3	76.3	0.67
Willow	77.8	53.9	0.50
Alder	92.3	92.3	0.92
Empetrum Dead	97.7	86.0	0.84
Mixed Forb	55.1	54.0	0.46
Sedge	49.1	71.1	0.65

The average total transformed divergence value across all vegetative classes was 1710, indicating that spectral separability was relatively high between most classes (Table 2.5). Empetrum, mixed forb, and sedge had the lowest overall average transformed divergence values (1523, 1593, and 1556 respectively), indicating poor separation within these classes. By comparison, alder and empetrum-dead had the highest overall average transformed divergence values (1996 and 1977, respectively), indicating good overall spectral separability. The lowest direct comparison of transformed divergence values between vegetative classes were between willow and empetrum, empetrum and sedge, sedge and mixed forb, and willow and mixed forb (1227, 979, 1250, and 1238, respectively). These classes had low transformed divergence due to the high similarity of spectral information reflected across the five RapidEye spectral bands (Figure 2.3). Generally, low transformed divergence values between classes correspond with misclassification between those classes (Table 2.6). Corresponding with the 4 lowest vegetative transformed divergence values, willow and empetrum, empetrum and sedge, sedge and mixed forb, and willow and mixed forb, also had the highest rates of misclassification (11.1%, 2.2%, 18.2%, and 7.4% respectively).

Table 2.5 Transformed divergence value matrix for vegetative land cover classes.

Cover Class	Empetrum	Willow	Alder	Empetrum - Dead	Mixed Forb	Sedge	Average Total
Empetrum	-	1227	1991	1937	1481	979	1523
Willow	1227	-	1989	2000	1238	1602	1611
Alder	1991	1989	-	2000	2000	1999	1996
Empetrum - Dead	1937	2000	2000	-	1998	1952	1977
Mixed Forb	1481	1238	2000	1998	-	1250	1593
Sedge	979	1602	1999	1952	1250	-	1556
Average Total	1523	1611	1996	1977	1593	1556	1710

Table 2.6 Error matrix showing classification accuracy and misclassification rate by class.

Cover Class	Empetrum		Willow		Barren Ground		Alder		Empetrum Dead		Mixed Forb		Sedge	
	Producers	Users	Producers	Users	Producers	Users	Producers	Users	Producers	Users	Producers	Users	Producers	Users
Water	0.0	0.0	0.0	0.0	0.0	29.2	0.0	3.8	0.0	0.0	0.0	0.0	0.0	0.0
Empetrum	76.3	76.3	11.1	5.1	5.6	0.0	3.8	3.8	2.3	12.0	20.4	22.0	10.9	5.3
Willow	2.2	3.2	77.8	53.8	0.0	0.0	3.8	0.0	0.0	0.0	6.1	4.0	21.8	2.6
Barren Ground	0.0	1.1	0.0	0.0	88.9	66.7	0.0	0.0	0.0	2.0	2.0	0.0	0.0	0.0
Alder	1.1	1.1	0.0	2.6	0.0	0.0	92.3	92.3	0.0	0.0	0.0	0.0	0.0	0.0
Empetrum Dead	6.5	1.1	0.0	0.0	5.6	0.0	0.0	0.0	97.7	86.0	0.0	0.0	0.0	0.0
Mixed Forb	11.8	10.8	7.4	7.7	0.0	4.2	0.0	0.0	0.0	0.0	55.1	54.0	18.2	21.1
Sedge	2.2	6.5	3.7	30.8	0.0	0.0	0.0	0.0	0.0	0.0	16.3	20.0	49.1	71.1
Total	100	100	100	100	100	100	100	100	100	100	100	100	100	100

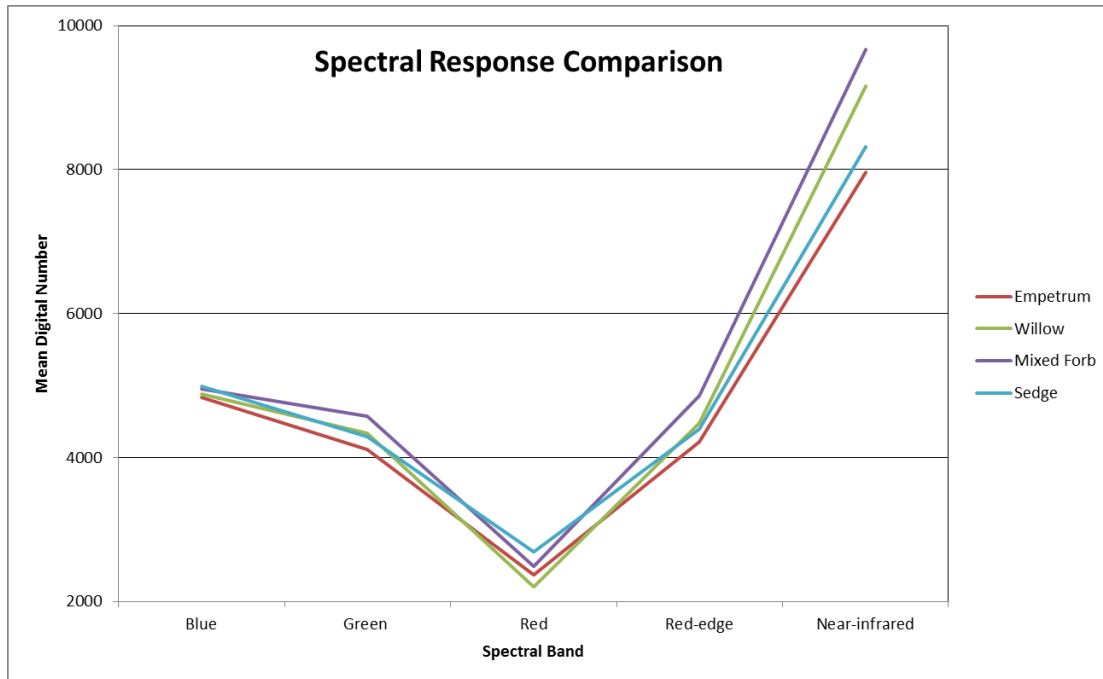


Figure 2.3 Spectral response patterns for 4 vegetative classes in the RapidEye maximum likelihood classification.

Red-edge Spectral Band Assessment

Accuracy assessments between all four RapidEye composite images showed that the original RapidEye image had the highest overall accuracy at 71.5% with a kappa statistic of 0.66 (Table 2.7).

Table 2.7 Comparison of overall classification accuracy and Kappa statistic for 4 RapidEye composite classifications.

RapidEye Composite Image	Overall Classification Accuracy (%)	Overall Kappa Statistic
RapidEye	71.56	0.66
RapidEye - RE	67.81	0.61
RapidEye + NDVI	69.38	0.63
RapidEye - RE + NDVI	65.63	0.59

The RapidEye – RE composite image had a lower overall accuracy rate (67.8%) and a kappa statistic of 0.61. Removing the red-edge spectral information reduced the accuracy in kappa by 0.05. The overall classification accuracy of the 6-band RapidEye + NDVI composite

image (69.4%) approached that of the original RapidEye image. The final two RapidEye composite images both had lower overall classification accuracy indicating that the NDVI band introduced spectral variability and confusion into the maximum likelihood supervised classification routine. The 5-band RapidEye – RE + NDVI composite image had the lowest overall classification accuracy between all 4 composite images at 65.6% with a kappa statistic of 0.59. The removal of the red-edge band and addition of the NDVI band resulted in a 0.07 reduction in the kappa statistic. The red-edge band and combinations of spectral bands in the RapidEye composite images affected the accuracy rate between vegetation classes (Figure 2.4, Table 2.8).

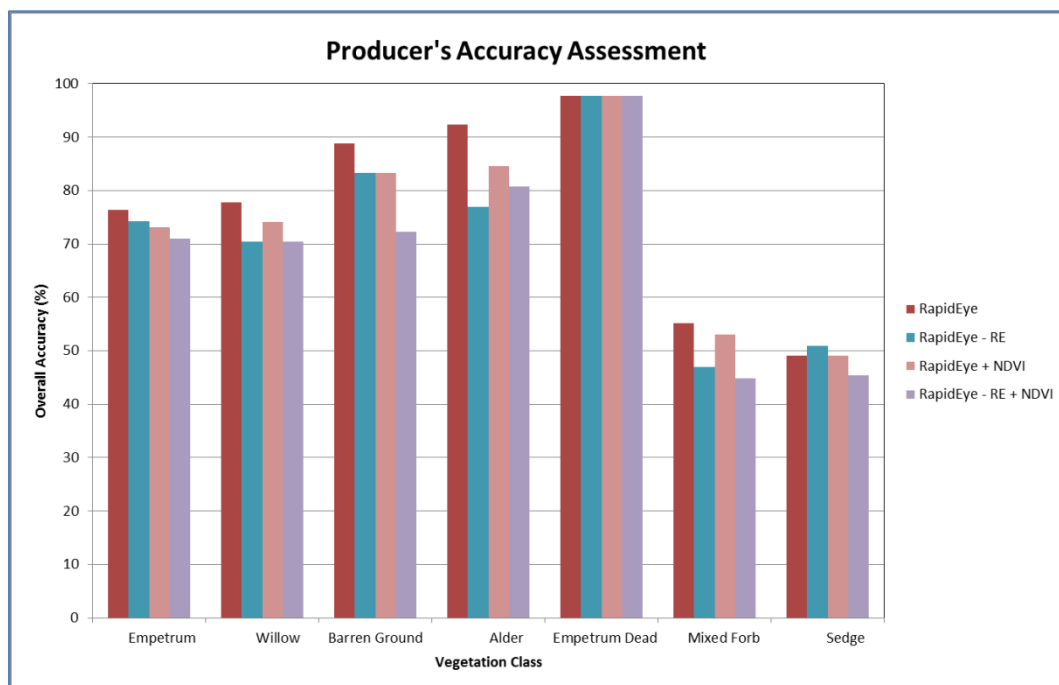


Figure 2.4 Producer's accuracy rate (%) for 7 vegetation classes between 4 RapidEye composite classifications.

Inclusion of the red-edge band increased the accuracy rate for nearly all vegetative classes. Percent deviation between the original RapidEye image and the RapidEye – RE composite image ranged from -3.57 % to 21.8 %. The alder vegetation class had the highest increase in User's and Producer's accuracy rate, 10.7 % and 20.0 % deviation respectively.

Table 2.8 User's and producer's accuracy rate comparison between RapidEye and RapidEye – RE composite image.

Cover Class	User's Accuracy			Producer's Accuracy		
	RapidEye	RapidEye - RE	Deviation (%)	RapidEye	RapidEye - RE	Deviation (%)
Empetrum	76.34	73.40	4.01	76.34	74.19	2.90
Willow	53.85	52.78	2.03	77.78	70.37	10.53
Barren Ground	66.67	68.18	-2.21	88.89	83.33	6.67
Alder	92.31	83.33	10.78	92.31	76.92	20.01
Empetrum Dead	86.00	86.00	0.00	97.73	97.73	0.00
Mixed Forb	54.00	53.49	0.95	55.10	46.94	17.38
Sedge	71.05	58.33	21.81	49.09	50.91	-3.57

Inclusion of the red-edge band increased overall spectral separability between composite images (Table 2.9). Average and minimum transformed divergence values increased slightly when the red-edge band was included in the composite image. Inclusion of the red-edge band was variable in increasing or decreasing the spectral separability between vegetation classes by band, indicating that the reflectance of red-edge information is species dependent (Table 2.10). Overall the red-edge band had the highest average transformed divergence value, 1405, while the blue spectral band had the lowest average transformed divergence value, 743. Select comparisons of transformed divergence between vegetative classes indicate that the red-edge band is variable in increasing the spectral separability between classes. General trends show that the red-edge band adds beneficial spectral information for distinguishing between vegetative classes when using a maximum likelihood classification.

Table 2.9 Transformed divergence spectral separability values for 4 RapidEye composite classificaions. Average, minimum, and select vegetative comparisons of transformed divergence values are listed.

RapidEye Composite Image	Average	Minimum	Willow:Alder	Willow:Sedge	Willow:Mixed Forb	Mixed Forb:Sedge
RapidEye	1903	979	1989	1602	1238	1250
RapidEye - RE	1885	788	1952	1513	1148	1074
RapidEye + NDVI	1957	1035	1993	1722	1995	1813
RapidEye - RE + NDVI	1949	863	1968	1955	1786	1429

Table 2.10 Transformed divergence values by band for select vegetative class comparisons in the original RapidEye classification.

Band	Ave	Min	Emp:Mixed Forb	Sedge:Willow	Sedge:Mixed Forb
Blue	743	51	251	438	51
Green	1257	69	1770	69	1023
Red	1326	256	256	1703	447
Red-edge	1405	69	1764	247	1358
Near-infrared	1102	64	1549	628	1220

Comparison to NLCD

The overall classification accuracy for the NLCD image was 39.7% with a kappa statistic of 0.19 (Table 2.11). The RapidEye recoded image for comparison to NLCD had a slightly higher accuracy rate compared to the original RapidEye classified image at 74.1%, with a kappa statistic of 0.64. The kappa statistic value was lower by 0.02 kappa compared to the original RapidEye image classification. This was due to the reduced number of classes, which results in a higher probability of chance agreement.

Table 2.11 Overall classification accuracy and kappa statistics for the RapidEye and NLCD land cover maps.

Land Cover Image	Overall Classification	
	Accuracy (%)	Kappa Statistic
RapidEye	74.1	0.64
NLCD	39.7	0.19

Comparison of the RapidEye land cover image to the NLCD image of Unimak Island showed that both NLCD and RapidEye were similar in spatial extent of land cover classes. Figure 2.5 shows an overview of Unimak Island with the RapidEye and the NLCD images representing the same land cover classes.

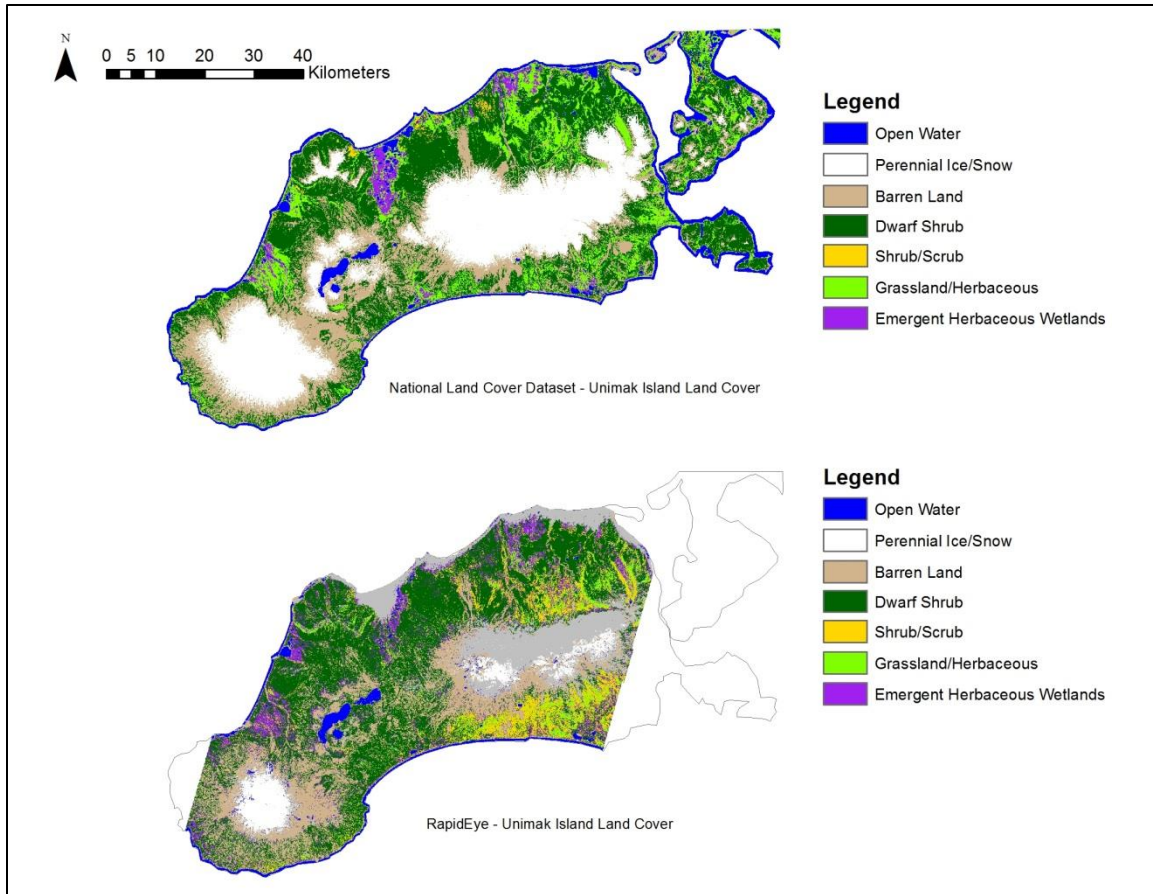


Figure 2.5 Overview of the NLCD and RapidEye land cover maps.

Generally, NLCD had similar coverage for the dwarf shrub, open water, barren land, and emergent herbaceous wetlands classes. A major difference is visible in the reduced area coverage of a shrub/scrub class for the NLCD on the southeastern side of Unimak Island, and the over estimation of the grassland/herbaceous class across the island.

Figure 2.6 shows a comparison of the difference in classified images between the NLCD and RapidEye images at the same scale and location. Evident is the difference in spatial resolution, (5m pixels RapidEye vs. 30m pixels Landsat), and the difference in class assignments. The NLCD image appears to overestimate the areal coverage of Grassland/Herbaceous class and underestimate the areal coverage of Shrub/Scrub and Emergent

Wetland Herbaceous classes. Dwarf shrub areal coverage remained very comparable to the empetrum classes between the two land cover maps.

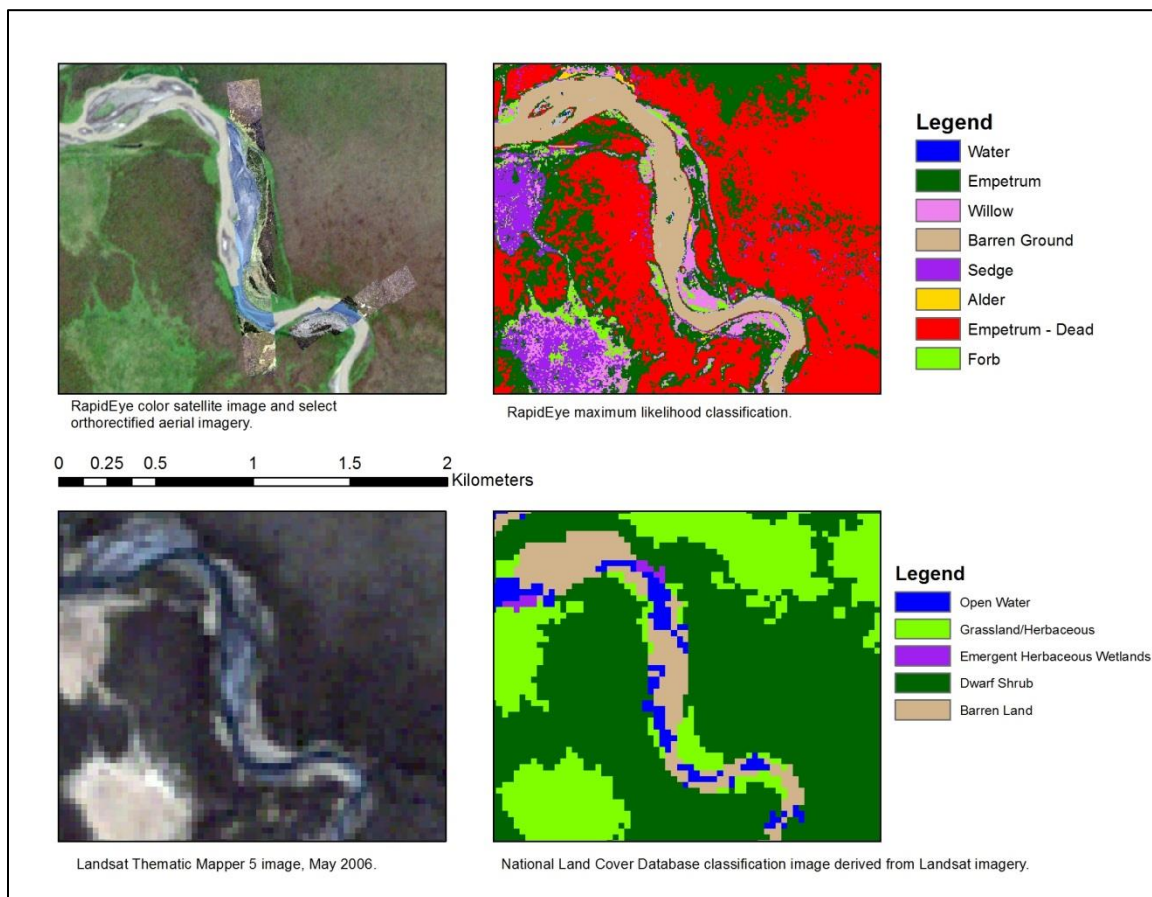


Figure 2.6 Comparison of RapidEye and Landsat NLCD land cover maps. The higher spatial resolution of RapidEye and the difference in classification can be seen.

These trends are supported as seen in the areal hectare coverage of classes in Table 2.12. Dwarf shrub and open water were the most similar in areal coverage, with only 9.9% and -17.5% difference relative to the RapidEye classified image. The NLCD shrub/scrub (combined alder/willow RapidEye) class was underestimated relative to the RapidEye classification. NLCD reported an areal coverage of 2,015 ha while RapidEye reported 26,114, a 92.3% difference. The emergent herbaceous wetlands cover class was also underestimated in the NLCD land cover map. NLCD reported 7,796 ha while RapidEye produced an estimate of 30,468 ha, a 74.4% difference.

Table 2.12 Areal coverage of shared land cover classes in RapidEye and NLCD land cover maps.

Class Name	RapidEye - Hectares	NLCD - Hectares	Percent Difference to RapidEye
Open Water	10,508	12,349	-17.5
Barren Land	40,933	77,085	-88.3
Dwarf Shrub	121,286	109,262	9.9
Shrub/Scrub	26,114	2,015	92.3
Grassland Herbaceous	16,772	35,482	-111.5
Emergent Herbaceous Wetlands	30,468	7,796	74.4

A RapidEye/NLCD matrix or difference image is displayed in Figure 2.7. The matrix image shows the areas of Unimak Island where shared land cover classes overlap between the RapidEye and NLCD classification images. Generally, areas and land cover classes that overlap are the empetrum and dwarf shrub classes along the north side of the island. Two classes that failed to overlap very well are the alder and willow classes, with the shrub/scrub class of the NLCD. Alder was dominant along the southeastern end of Unimak Island, and is visibly absent as a shrub/scrub class in the NLCD.

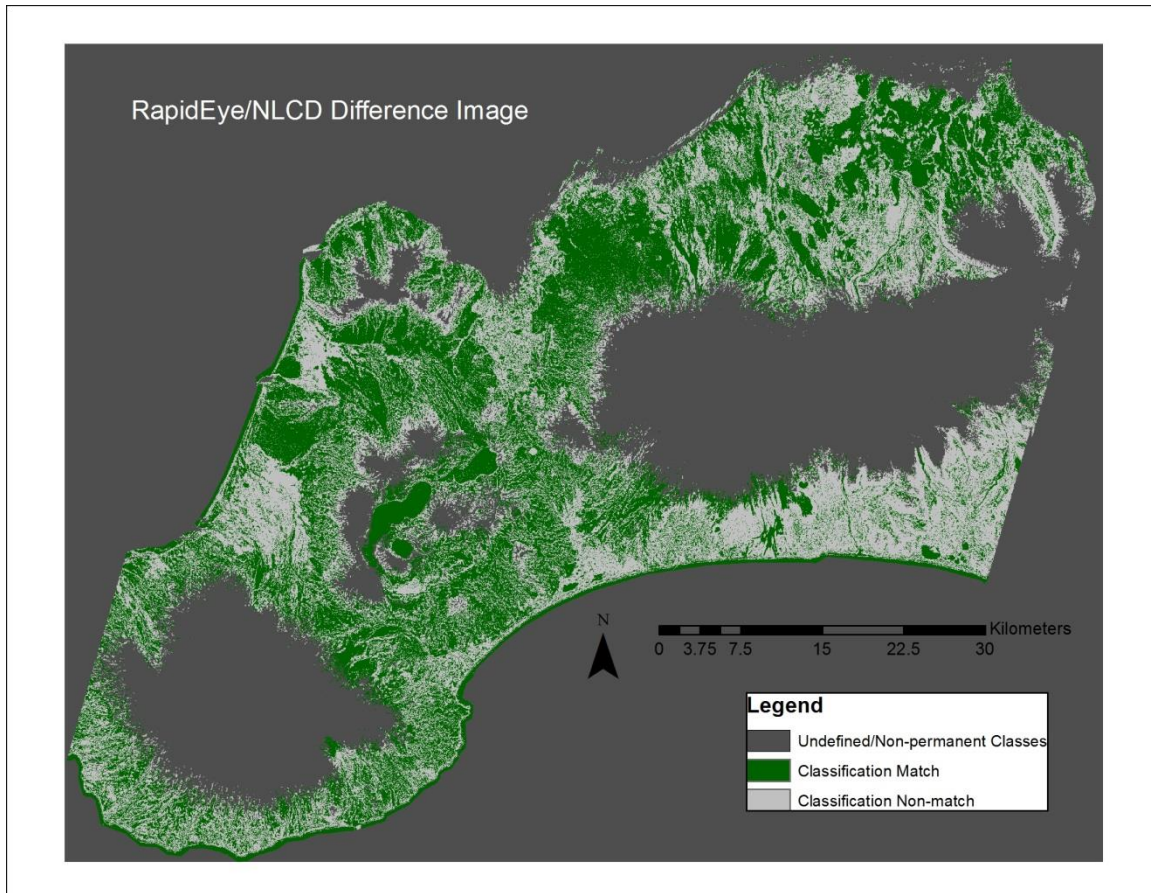


Figure 2.7 Image difference between Rapideye and NLCD land cover maps. Green pixels show areas of overlapping matching classes, while light-grey pixels indicate overlapping areas where the classification produced different classes.

DISCUSSION

RapidEye is a new, relatively inexpensive multi-spectral high resolution remote sensing platform with a global temporal resolution of 1 day. Accuracy rates of 71.5% were achieved when this imagery was used in a supervised classification routine. This accuracy rate was similar to but slightly less than that of other land cover maps produced using RapidEye (Schuster et al., 2012; Tapsall et al., 2010; Tigges et al., 2013). Only 90% of the land surface of Unimak Island was classified due to cloud cover and the narrow swath width of the RapidEye sensor. *Empetrum nigrum* vegetation communities were the most widespread across the island at approximately over 70% of total vegetation land coverage. Willow communities, an important forage species of

caribou was estimated to be as 7.1% of the total vegetation cover percentage. A basic land cover map for use with wildlife management is an important basis for ecological studies. Previously no land cover maps of Unimak Island have included this definition of vegetative classes.

Red-edge Spectral Band Assessment

The red-edge spectral band (690 – 730 nm) is a new commercially available band of spectral information of for use with land cover mapping. We found that the inclusion of this band provided additional spectral information that boosted overall classification accuracy rates when used with a maximum likelihood classification routine. When a composite image was created substituting an NDVI band for the red-edge band, classification accuracy decreased. This indicates that the NDVI band provides different spectral information compared to the red-edge band, and cannot be simply substituted in its place. Additionally, the inclusion of an NDVI band increased the spectral separability between most vegetation classes, but failed to increase the overall accuracy of the classification. This could be due to increased variability between classes with the addition of the NDVI spectral information. Very similar results were seen with a composite image assessment using RapidEye to test the effects of land cover accuracy when including and excluding the red-edge band. Schuster et al. (2012) found that including the red-edge band increased accuracy of land cover assessments, while creating a composite image with an additional spectral band, NDVI, decreased classification accuracy. For the comparison between the two RapidEye NDVI composite images, the 6-band NDVI composite image which included the red-edge band had higher classification accuracy than the 5-band NDVI composite image which excluded the red-edge band. This was similar to the accuracy increase seen in the first set of RapidEye composite imagery comparisons without the NDVI band. This further

indicates that the red-edge band provides beneficial spectral information for increasing classification accuracy.

The highest increase in accuracy when including the red-edge band came from the alder, mixed forb, and sedge classes. Schuster et al., 2012 also found similar results with the highest increase in accuracy coming from bush vegetation and herbaceous perennial plants.

Comparison to NLCD

Large differences were observed between the RapidEye and NLCD land cover maps both in overall accuracy, and the areal coverage of each land cover class. Overall accuracy of the RapidEye land cover map was 60% higher than that of the overall accuracy of the NLCD land cover map. Comparisons between the differences in vegetative class areal coverage between these two land cover maps ranged from 9.9% to -111.5% relative to RapidEye. Differences between the overall accuracy can be attributed to the difference in spatial resolution, to the addition of the red-edge spectral band, and to the difference in timing of the date of imagery acquisition. The increase in accuracy due to these factors is not known, and should be looked into further. It is probable that the majority of the difference in accuracy rate is due the higher spatial resolution of the RapidEye imagery. Previous studies have found that higher spatial resolution can improve the accuracy of land cover classifications (Cushine, 1987). Many vegetative communities on Unimak Island are smaller than the 900 m² area of the Landsat pixel and were not accurately classified. This could change using sub-pixel classification techniques. Imagery acquisition date affects the spectral response patterns of vegetation and thus the spectral separability of those vegetative classes. The Landsat image that was based on the NLCD was acquired in May 2006, vegetation at this time of year had yet to leaf out and spectral difference

between vegetative communities were less pronounced than later in the year. Generally, fall dates of imagery acquisition are thought to provide the highest degree of spectral separability and provide higher accuracy due to the senescence of vegetation (Schrieffer & Congalton, 1995; Walton, 2009).

Implications

We have shown that RapidEye imagery can be used to produce a highly accurate land cover map at a high spatial resolution. Land cover classifications are important for ecological studies and often form the basis for such studies. For caribou and large animal management, a vegetation map that includes vegetation classes that normally appear at a fine resolution is important to assess habitat abundance and quality, which is difficult with a lower resolution satellite platform. RapidEye may prove to be a valuable tool for multi-spectral remote sensing, especially in areas of high cloud cover, such as in the Aleutian Islands and the Alaskan Peninsula of Alaska.

Improvements and Future Research Areas

Our classification and accuracy assessment of RapidEye imagery show that high spatial resolution is an important factor in order to classify vegetation that occupy a small spatial scale or are spatially non-contiguous. The orthorectified RapidEye imagery was displaced by up to 30 meters or 6 RapidEye pixels in relation to orthorectified aerial imagery. Many vegetative communities on Unimak Island occupy only several RapidEye pixels; small orthorectification errors can introduce a high error rate into accuracy assessments. We assume that for our accuracy assessments the effects of orthorectification errors were reduced due to the spatial adjustment of

our high resolution aerial imagery, but this should still be considered as a major source of error. A further source of error may be misregistration between RapidEye bands. Spectral information is collected using 5 separate CCD arrays on the RapidEye satellite platform. Co-registration between bands using a DEM and an auto-correlation statistical method results in a co-registration accuracy between bands of less than 0.2 pixels, ERDAS Imagine[®]. Misregistration between bands was evident in areas of high contrast such as remnant snow cover, with band displacement being up to 4-5 pixels in some areas. While for the majority of the RapidEye image an assessment of band misregistration could not be estimated, misregistration could insert a high degree of error into classifications. We can assume that both forms of misregistration would affect classifications and accuracy assessments. Further research should be undertaken to assess the true effect of orthorectification and band misregistration errors on classification accuracy.

Timing of imagery acquisition also has a major impact on classification accuracy. We found through multiple date repeat aerial imagery, that vegetation classes on Unimak Island were the most spectrally distinct during the summer period of imagery acquisition. RapidEye imagery was acquired between the summer and fall time periods, and appeared to classify out differences between vegetative groups well. Further research should look more closely at the phenological differences in imagery acquisition time and the resulting classification accuracy.

LITERATURE CITED

- Bartsch, A., Kumpula, T., Forbes, B. C., & Stammer, F. (2010). Detection of snow surface thawing and refreezing in the Eurasian Arctic with QuikSCAT: implications for reindeer herding. *Ecological Applications : A Publication of the Ecological Society of America*, 20(8), 2346–58.
- Cohen, W. B., & Goward, S. N. (2004). Landsat's Role in Ecological Applications of Remote Sensing. *BioScience*, 54(6), 535–545.
- Congalton, R. G. (1991). A Review of Assessing the Accuracy of Classifications of Remotely Sensed Data. *Remote Sensing of Environment*, 46, 35–46.
- Cushine, J. L. (1987). The interactive effect of spatial resolution and degree of internal variability within land-cover types on classification accuracies. *International Journal of Remote Sensing*, 8(1), 15–29.
- Dale, B., Webber, M., Butler, L., Collins, W. B., Spalinger, D. E., Hundertmark, K., Martin, J., Watts, D., & Adams, L. G. (2013). *Population dynamics, genetics, and habitat characteristics of the Unimak Island Caribou Herd*.
- Eitel, J. U. H., Vierling, L. A., Litvak, M. E., Long, D. S., Schulthess, U., Ager, A. A., Krofcheck, D. J., Stoscheck, L. (2011). Broadband, red-edge information from satellites improves early stress detection in a New Mexico conifer woodland. *Remote Sensing of Environment*, 115(12), 3640–3646.
- Fancy, S. G., Pank, L. F., Whitten, K. R., & Regelin, W. L. (1989). Seasonal movements of caribou in arctic Alaska as determined by satellite. *Canadian Journal of Zoology*, 67(3), 644–650.
- Fry, J., Xian, G., Jin, S., Dewitz, J., Homer, C., Yang, L., ... Wickham, J. (2011). Completion of the 2006 National Land Cover Database for the Conterminous United States. *PE&RS*, 77(9), 858–864.
- Gordon, I. J., Hester, A. J., & Festa-Bianchet, M. (2004). REVIEW: The management of wild large herbivores to meet economic, conservation and environmental objectives. *Journal of Applied Ecology*, 41(6), 1021–1031.
- Hansen, M., Franklin, S., Woudsma, C., & Peterson, M. (2001). Caribou habitat mapping and fragmentation analysis using Landsat MSS, TM, and GIS data in the North Columbia Mountains, British Columbia, Canada. *Remote Sensing of Environment*, 77(1), 50–65.
- Heggberget, T. M., Gaare, E., & Ball, J. P. (2010). Reindeer (*Rangifer tarandus*) and climate change: importance of winter forage. *Rangifer*, 22(1), 13–31.

- Jensen, J. R. (1996). *Remote Sensing of the Environment: An Earth Resource Perspective* (2nd ed., p. 316). Englewood Cliffs, NY, USA: Prentice Hall.
- Johnson, C. (2003). Characterizing woodland caribou habitat in sub-boreal and boreal forests. *Forest Ecology and Management*, 180(1-3), 241–248.
- Johnson, C. J., Parker, K. L., Heard, D. C., & Gillingham, M. P. (2002). Movement parameters of ungulates and scale-specific responses to the environment. *Journal of Animal Ecology*, 71(2), 225–235.
- Johnson, C., Parker, K., & Heard, D. (2001). Foraging across a variable landscape: behavioral decisions made by woodland caribou at multiple spatial scales. *Oecologia*, 127(4), 590–602.
- Kokaly, R. F., Asner, G. P., Ollinger, S. V., Martin, M. E., & Wessman, C. a. (2009). Characterizing canopy biochemistry from imaging spectroscopy and its application to ecosystem studies. *Remote Sensing of Environment*, 113, S78–S91.
- LDP LLC (2014) at <http://www.maxmax.com> (last accessed 25 June 2014)
- Mårell, A., & Edenius, L. (2006). Spatial heterogeneity and hierarchical feeding habitat selection by reindeer. *Arctic, Antarctic, and Alpine Research*, 38(3), 413–420.
- Markham, B. L., Storey, J. C., Williams, D. L., & Irons, J. R. (2004). Landsat sensor performance: history and current status. *IEEE Transactions on Geoscience and Remote Sensing*, 42(12), 2691–2694.
- Post, E., & Forchhammer, M. C. (2008). Climate change reduces reproductive success of an Arctic herbivore through trophic mismatch. *Philosophical Transactions of the Royal Society of London. Series B, Biological Sciences*, 363(1501), 2369–75.
- Post, E., Pedersen, C., Wilmers, C. C., & Forchhammer, M. C. (2008). Warming, plant phenology and the spatial dimension of trophic mismatch for large herbivores. *Proceedings. Biological Sciences / The Royal Society*, 275(1646), 2005–13.
- Schriever, J. R., & Congalton, R. G. (1995). Evaluating Season Variability as an Aid to Cover-Type Mapping from Landsat Thematic Mapper Data in the Northeast. *Photogrammetric Engineering and Remote Sensing*, 61(3), 321–327.
- Schuster, C., Förster, M., & Kleinschmit, B. (2012). Testing the red edge channel for improving land-use classifications based on high-resolution multi-spectral satellite data. *International Journal of Remote Sensing*, 33(17), 5583–5599.
- Shipley, L. A., & Spalinger, D. E. (1992). Mechanics of browsing in dense food patches: effects of plant and animal morphology on intake rate. *Canadian Journal of Zoology*, 70(9), 1743–1752.

- Stien, A., Loe, L. E., Mysterud, A., Severinsen, T., Kohler, J., & Langvatn, R. (2010). Icing events trigger range displacement in a high-arctic ungulate. *Ecology*, 91(3), 915–20.
- Story, M., & Congalton, R.G. 1986. Accuracy assessment: a user's perspective. *Photogrammetric Engineering and Remote Sensing*, 52: 397-399.
- Talbot, S. S., Talbot, S. L., & Schofield, W. B. (2006, October). Vascular flora of Izembek National Wildlife Refuge, Westernmost Alaska Peninsula, Alaska. *Rhodora*.
- Tapsall, B., Milenov, P., & Tas, K. (2010). Analysis of RapidEye imagery for annual landcover mapping as an aid to European Union (EU) Common Agricultural Policy. In *ISPRS TC VII Symposium* (Vol. XXXVIII, pp. 568–573).
- Théau, J., Peddle, D. R., & Duguay, C. R. (2005). Mapping lichen in a caribou habitat of Northern Quebec, Canada, using an enhancement-classification method and spectral mixture analysis. *Remote Sensing of Environment*, 94(2), 232–243.
- Tigges, J., Lakes, T., & Hostert, P. (2013). Urban vegetation classification: Benefits of multitemporal RapidEye satellite data. *Remote Sensing of Environment*, 136, 66–75.
- Trudell, J., & White, R. G. (1981). The Effect of Forage Structure and Availability on Food Intake , Biting Rate , Bite Size and Daily Eating Time of Reindeer. *Journal of Applied Ecology*, 18(1), 63–81.
- Tyler, N. J. C. (2010). Climate, snow, ice, crashes, and declines in populations of reindeer and caribou (*Rangifer tarandus* L.). *Ecological Monographs*, 80(2), 197–219.
- U.S. Fish and Wildlife Service. (2010). *Management Alternatives for the Unimak Island Caribou Herd: Environmental Assessment* (pp. 1–94).
- Ustin, S. L., Gitelson, A. A., Jacquemoud, S., Schaepman, M., Asner, G. P., Gamon, J. A., & Zarco-Tejada, P. (2009). Retrieval of foliar information about plant pigment systems from high resolution spectroscopy. *Remote Sensing of Environment*, 113, S67–S77.
- Viereck, L. A., Dyrness, C. T., & Batten, A. R. (1992). *The Alaska Vegetation Classification*.
- Vors, L. S., & Boyce, M. S. (2009). Global declines of caribou and reindeer. *Global Change Biology*, 15(11), 2626–2633.
- Walton, K. M. 2009. Landscape scale quantification of wildlife habitat using hierarchical classification techniques. Thesis. University of Alaska Anchorage, Anchorage, USA.
- Walton, K., Spalinger, D. E., Harris, N. R., Collins, W. B., & Willacker, J. J. (2011). Landscape Scale Quantification of Wildlife Habitat using Landsat Imagery and Hierarchical Classification Techniques. *Submitted*.

- Walton, K. M., Spalinger, D. E., Harris, N. R., Collins, W. B. and Willacker, J. J. (2013), High spatial resolution vegetation mapping for assessment of wildlife habitat. *Wildlife Society Bulletin*, 37: 906–915.
- White, R.G. 1983. Foraging patterns and their multiplier effects on productivity of northern ungulates. *Oikos* 40(3):377-384.
- White, R.G. and J. Trudell. 1980. Habitat Preference and Forage Consumption by Reindeer and Caribou near Atkasook, Alaska. *Arctic and Alpine Research* 12(4):511-529.
- Xie, Y., Sha, Z., & Yu, M. (2008). Remote sensing imagery in vegetation mapping: a review. *Journal of Plant Ecology*, 1(1), 9–23.

GENERAL CONCLUSIONS

Trends of population decline for caribou herds across the circumpolar north may be related to extreme weather events associated with climate change through impacts on forage quality (Post & Forchhammer, 2008; Post et al., 2008) and winter forage availability (Heggberget et al., 2010; Stien et al., 2010; Tyler, 2010). The Unimak Island caribou herd is an isolated herd in a moderate maritime environment that may or may not be affected by these global climate changes, but has experienced a dramatic decrease in the herd's population similar to other Southwestern Alaskan caribou herds (U.S. Fish and Wildlife Service, 2010, Valkenburg et al., 2003). The spatial distribution of forage for large herbivores is a key component to assess the role of climate change and forage quality on caribou population dynamics (Mårell & Edenius, 2006). Very little was known about the forage spatial distribution due to the extremely high cloud cover and frequent inclement weather of the region, limiting both remotely sensed data acquisition and on-the-ground forage data collection (Valkenburg et al., 2003). In this study we developed and assessed the use of two remote sensing techniques for creating caribou forage maps.

We first evaluated the use of low-level high spatial resolution aerial imagery at 3 distinct phenological time periods on Unimak Island using color and infrared digital photography for developing caribou habitat maps. We found that contrary to our expectations, the fall time period, or senescence, was not the most spectrally distinct and that the summer time period, or peak photosynthetic activity, was the most distinct. Fall and spring time periods were relatively similar, with an accuracy assessment of approximately 78%. The summer time period accuracy assessment was approximately 84%. These rates of accuracy were similar to other studies using aerial imagery for creating land cover maps in Alaska for large herbivores (Walton et al., 2013).

We also looked at transformed divergence values and spectral separability between vegetative classes, spectral bands and date of imagery acquisition. We found that transformed divergence values were the highest for the summer time period, which corresponds to the highest accuracy across the 3 sampled time periods, but generally disagrees with other studies that found fall senescence to have the highest spectral separability (Schriever & Congalton, 1995).

Secondly, we evaluated the use of multi-spectral satellite imagery from the relatively new satellite imagery acquisition company RapidEye for use with creating caribou habitat maps. We found that this source of satellite imagery provided a highly accurate land cover map, similar to other land cover maps produced using RapidEye imagery (Schuster et al., 2012; Tapsall et al., 2010; Tigges et al., 2013). The red-edge band of RapidEye imagery was shown to provide additional spectral information that was useful in increasing the accuracy of land cover maps produced using maximum likelihood classifications, similar to a previous study assessing the red-edge band in RapidEye (Schuster et al., 2012). Finally RapidEye was compared to the NLCD dataset, and was found to have a much higher accuracy rate while including a higher class definition (74.1% accuracy vs. 39.7% accuracy).

Overall, we found that both aerial imagery and RapidEye satellite imagery provide an excellent means to creating land cover maps for use with caribou forage management purposes. Each provides relatively high spatial resolution for a detailed approach to determining spatial distribution of forage plants. This is important for caribou management because the distribution of forage plants can be quite heterogeneous across the landscape, and fine resolution imagery makes it possible to delineate important forage species for caribou that tend to exist on a small spatial scale, such as willow. Furthermore, both aerial and RapidEye satellite imagery have a

relatively high temporal resolution, allowing for a higher chance of cloud-free data acquisition given the high cloud cover of the Southern Alaska Peninsula and the Aleutian Islands.

It is not known whether the fall senescence period was completely missed on Unimak Island with respect to the fall sampling of aerial imagery. Further research should look at a finer detailed temporal sampling scheme for capturing phenological time periods in order to assess the effect of phenology and spectral reflectance of vegetation. We found the red-edge band of RapidEye to provide additional spectral information that boosted classification accuracy. It is not known whether this effect is due to differences in red-edge reflectance between vegetation classes. Further research should look specifically at the differences in red-edge reflectance in these vegetation community types.

LITERATURE CITED

- Dale, B., Webber, M., Butler, L., Collins, W. B., Spalinger, D. E., Hundertmark, K., Martin, J., Watts, D., & Adams, L. G. (2013). *Population dynamics, genetics, and habitat characteristics of the Unimak Island Caribou Herd*.
- Heggberget, T. M., Gaare, E., & Ball, J. P. (2010). Reindeer (*Rangifer tarandus*) and climate change: importance of winter forage. *Rangifer*, 22(1), 13–31.
- Klein, D. R. (1991). Limiting factors in caribou population ecology. *Rangifer*, (7), 30–35.
- Mårell, A., & Edenius, L. (2006). Spatial heterogeneity and hierarchical feeding habitat selection by reindeer. *Arctic, Antarctic, and Alpine Research*, 38(3), 413–420.
- McArt, S. H., Spalinger, D. E., Collins, W. B., Schoen, E. R., Stevenson, T., & Bucho, M. (2009). Summer dietary nitrogen availability as a potential bottom-up constraint on moose in south-central Alaska. *Ecology*, 90(5), 1400–11.
- Post, E., & Forchhammer, M. C. (2008). Climate change reduces reproductive success of an Arctic herbivore through trophic mismatch. *Philosophical Transactions of the Royal Society of London. Series B, Biological Sciences*, 363(1501), 2369–75.
- Post, E., Pedersen, C., Wilmers, C. C., & Forchhammer, M. C. (2008). Warming, plant phenology and the spatial dimension of trophic mismatch for large herbivores. *Proceedings. Biological Sciences / The Royal Society*, 275(1646), 2005–13.
- Sæther, B. (1997). Environmental stochasticity and population dynamics of large herbivores: a search for mechanisms. *Trends in Ecology & Evolution*, 12(4), 143–149.
- Schriever, J. R., & Congalton, R. G. (1995). Evaluating Season Variability as an Aid to Cover-Type Mapping from Landsat Thematic Mapper Data in the Northeast. *Photogrammetric Engineering and Remote Sensing*, 61(3), 321–327.
- Schuster, C., Förster, M., & Kleinschmit, B. (2012). Testing the red edge channel for improving land-use classifications based on high-resolution multi-spectral satellite data. *International Journal of Remote Sensing*, 33(17), 5583–5599.
- Stien, A., Loe, L. E., Mysterud, A., Severinsen, T., Kohler, J., & Langvatn, R. (2010). Icing events trigger range displacement in a high-arctic ungulate. *Ecology*, 91(3), 915–20.
- Tapsall, B., Milenov, P., & Tas, K. (2010). Analysis of RapidEye imagery for annual landcover mapping as an aid to European Union (EU) Common Agricultural Policy. In *ISPRS TC VII Symposium* (Vol. XXXVIII, pp. 568–573).
- Tigges, J., Lakes, T., & Hostert, P. (2013). Urban vegetation classification: Benefits of multitemporal RapidEye satellite data. *Remote Sensing of Environment*, 136, 66–75.

- Tyler, N. J. C. (2010). Climate, snow, ice, crashes, and declines in populations of reindeer and caribou (*Rangifer tarandus* L.). *Ecological Monographs*, 80(2), 197–219.
- U.S. Fish and Wildlife Service. (2010). *Management Alternatives for the Unimak Island Caribou Herd: Environmental Assessment* (pp. 1–94).
- Valkenburg, P., Sellers, R. A. R., Squibb, R. C. R., Woolington, J. D., Aderman, A. R., & Dale, B. W. (2003). Population dynamics of caribou herds in southwestern Alaska. *Rangifer*, 23(5), 131–142.
- Vors, L. S., & Boyce, M. S. (2009). Global declines of caribou and reindeer. *Global Change Biology*, 15(11), 2626–2633.
- Walton, K. M., Spalinger, D. E., Harris, N. R., Collins, W. B. and Willacker, J. J. (2013), High spatial resolution vegetation mapping for assessment of wildlife habitat. *Wildlife Society Bulletin*, 37: 906–915.

APPENDIX

Table A-1 Vegetative pairwise comparison of transformed divergence values by spectral band for Rapideye classification map.

Veg Class Comparison	Spectral Band				
	Blue	Green	Red	Red-edge	Near-infrared
Emp:Forb	251	1770	256	1764	1549
Emp:Willow	302	789	470	787	1073
Emp:Alder	962	1731	1906	1770	743
Emp:Sedge	265	502	1005	254	119
Forb:Willow	219	838	1100	1302	308
Forb:Alder	1494	2000	1977	2000	471
Forb:Sedge	51	1023	447	1358	1220
Willow:Alder	1185	1987	1592	1992	64
Willow:Sedge	438	69	1703	247	628
Alder:Sedge	1581	1965	1999	1953	350

Table A-2 Classification matrix (%) of NLCD class areas in common with RapidEye land cover map.

Cover Class	Open Water	Barren Land	Dwarf Shrub	Shrub/Scrub	Grassland/ Herbaceous	Emergent Herbaceous Wetlands
Open Water	77.3	0.8	0.1	0.3	0.2	1.5
Barren Land	15.4	45.5	2.5	0.8	1.1	2.8
Dwarf Shrub	3.6	36.5	70.3	77.7	29.1	43.2
Shrub/Scrub	1.1	6.6	11.9	6.0	19.8	10.7
Grassland/Herbaceous	0.4	4.1	6.5	2.1	16.0	6.7
Emergent Herbaceous Wetlands	2.2	6.5	8.7	13.3	33.8	35.2
Total	100	100	100	100	100	100

Table A-3 Classification matrix (hectares) of NLCD class areas in common with RapidEye land cover map.

Cover Class	Open Water	Barren Land	Dwarf Shrub	Shrub/Scrub	Grassland/ Herbaceous	Emergent Herbaceous Wetlands
Open Water	9,330	623	58	5	81	112
Barren Land	1,857	34,146	2,722	15	385	214
Dwarf Shrub	435	27,333	76,263	1,549	10,210	3,324
Shrub/Scrub	133	4,926	12,906	120	6,945	824
Grassland/Herbaceous	49	3,082	7,018	41	5,617	514
Emergent Herbaceous Wetlands	269	4,876	9,484	264	11,869	2,714
Total	12,072	74,987	108,452	1,995	35,107	7,702